Opioid Receptor Three-Dimensional Structures from Distance Geometry Calculations with Hydrogen Bonding Constraints

Irina D. Pogozheva, Andrei L. Lomize, and Henry I. Mosberg
College of Pharmacy, University of Michigan, Ann Arbor, Michigan 48109 USA

ABSTRACT   Three-dimensional structures of the transmembrane, seven α-helical domains and extracellular loops of δ, μ, and κ opioid receptors, were calculated using the distance geometry algorithm, with hydrogen bonding constraints based on the previously developed general model of the transmembrane α-bundle for rhodopsin-like G-protein coupled receptors (*Biophys. J.* 1997. 70:1963). Each calculated opioid receptor structure has an extensive network of interhelical hydrogen bonds and a ligand-binding crevice that is partially covered by a β-hairpin formed by the second extracellular loop. The binding cavities consist of an inner "conserved region" composed of 18 residues that are identical in δ, μ, and κ opioid receptors, and a peripheral "variable region," composed of 19 residues that are different in δ, μ, and κ subtypes and are responsible for the subtype specificity of various ligands. Sixteen δ-, μ-, or κ-selective, conformationally constrained peptide and nonpeptide opioid agonists and antagonists and affinity labels were fit into the binding pockets of the opioid receptors. All ligands considered have a similar spatial arrangement in the receptors, with the tyramine moiety of alkaloids or Tyr[1] of opioid peptides interacting with conserved residues in the bottom of the pocket and the tyramine N$^+$ and OH groups forming ionic interactions or H-bonds with a conserved aspartate from helix III and a conserved histidine from helix VI, respectively. The central, conformationally constrained fragments of the opioids (the disulfide-bridged cycles of the peptides and various ring structures in the nonpeptide ligands) are oriented approximately perpendicular to the tyramine and directed toward the extracellular surface. The results obtained are qualitatively consistent with ligand affinities, cross-linking studies, and mutagenesis data.

INTRODUCTION

Three different types of opioid receptors (δ, μ, and κ), identified based on their pharmacological properties, have recently been cloned (see reviews: Reisine, 1995; Dhawan et al., 1996; Zaki et al., 1996) and assigned to the large superfamily of rhodopsin-like G protein-coupled receptors (GPCRs). This superfamily of GPCRs consists of integral membrane proteins that transduce optical and chemical signals across the cellular membrane (Watson and Arkinstall, 1994) and share a common 3D structure. The seven-helical structure of the transmembrane domain has recently been demonstrated by electron cryomicroscopy (EM) studies of bovine, frog, and squid rhodopsins with a resolution of 6–9 Å (Schertler et al., 1993; Unger and Schertler, 1995; Unger et al., 1997; Davies et al., 1996). Many members of the GPCR family, especially rhodopsin, have been extensively studied by site-directed mutagenesis and a variety of physicochemical methods. These experimental data and the analysis of variability and hydrophobicity patterns in amino acid sequences of GPCRs have made it possible to assign the transmembrane helices of GPCRs to the peaks in the rhodopsin EM maps (Baldwin, 1993), and to construct a number of different approximate GPCR models (see reviews: Ballesteros and Weinstein, 1995; Donnelly et al., 1994). Some of these models have been built from the structure of

the nonhomologous 7-α-bundle membrane protein, bacteriorhodopsin (Henderson et al., 1990), whereas others have used the low-resolution rhodopsin EM maps and a few experimentally derived constraints to pack together seven "ideal" helices with arbitrarily chosen side-chain conformers (for example, Baldwin, 1997; Donnelly et al., 1994; Herzyk and Hubbard, 1995). The calculation of a more precise, atomic-level structure requires refinement of the spatial positions of entire helices, determination of their precise geometry, as helices are never "ideal" in proteins (Barlow and Thornton, 1988), and careful attention to side-chain packing.

To refine the structure of the transmembrane domain, we have developed and recently described a novel modeling approach that is based on the presence of numerous polar residues in the hydrophobic, lipid-embedded α-helices of GPCRs (Pogozheva et al., 1997). It is known that water-inaccessible polar groups of proteins have a strong tendency to form H-bonds (McDonald and Thornton, 1994). In transmembrane α-helices, peptide backbone groups are already paired, whereas the polar side chains must interact with each other to form intra- or interhelical H-bonds. The candidate H-bonding pairs can be identified from the analysis of sequence alignments as polar residues in intramembrane segments that appear and disappear simultaneously in various GPCRs. The corresponding H-bonds can then be used as constraints for packing the seven α-helical fragments by distance geometry calculations. Moreover, the side-chain H-bonds from many different GPCRs can be combined to increase the number of simultaneously applied constraints and to calculate an "average" 7-α-bundle structure. The

computational procedure was organized as an iterative refinement with evolving constraints that begins from an initial model of the α-bundle and continues until each buried polar side chain of each of the 410 GPCRs considered can participate in at least one hydrogen bond in the final structure (the root mean square deviation, r.m.s.d., between the initial and final structures was ~4 Å) (Pogozheva et al., 1997). This "saturation of hydrogen bonding potential" (McDonald and Thornton, 1994) criterion was very sensitive to structural mistakes during the refinement procedure. The transmembrane segments of individual GPCRs are hydrophobic and contain less than 30% polar residues, but when 410 different amino acid sequences are simultaneously considered, all interhelical contacts within the α-bundle are "labeled" by polar side chains forming intramolecular H-bonds. Displacement of any α-helix from its correct position breaks some H-bonds, producing unpaired polar side chains within the lipid bilayer in tens or hundreds of GPCRs.

The "average" atomic structure of the α-bundle has been tested by using it as a template to calculate the transmembrane domains of specific GPCRs whose H-bonds and close packing of nonpolar side chains must be compatible with the same common structure. The models of 28 different GPCRs (including vertebrate and invertebrate rhodopsins and a number of opioid, chemokine, glycoprotein, cationic amine, melatonin, and purine receptors) were generated by distance geometry, using H-bonds specific to each receptor, while using the "average" model to restrain the spatial positions of the helices. Analysis of the GPCR models reveals many features that are responsible for structural stability of the transmembrane α-bundle, such as the formation of extensive networks of interhelical H-bonds, aromatic and sulfur-aromatic clusters that are spatially organized as "polarity gradients," close packing of side chains throughout the transmembrane domain, and the formation of interhelical disulfide bonds in many GPCRs (Lomize et al., 1998). Some other features of the models are related to biological function and evolution of GPCRs, such as the formation of a spatially continuous "minicore" of 43 evolutionarily conserved residues, a multitude of correlated replacements of residues buried within the core, a Na^+ binding site, and complementarity of receptor binding pockets to many structurally dissimilar, conformationally constrained ligands (Lomize et al., 1998).

As has previously been discussed (Pogozheva et al., 1997; Lomize et al., 1998), the GPCR models obtained are consistent with a large body of experimental data that were not used in deriving the models and that therefore can serve as an independent control. The model of rhodopsin, for example (1boj and 1bok Protein Data Bank files), is in agreement with the arrangement of α-helices in the low-resolution 3D EM maps; mapping of water- and lipid-accessible rhodopsin residues by chemical probes; identification of residues surrounding retinal by site-directed mutagenesis and cross-linking; the orientations of all-*trans* and 11-*cis* retinal relative to the membrane plane and the

distances from the ligand to the intra- and extracellular surfaces, determined by linear dichroism and fluorescence quenching; reconstitution studies of opsin with synthetic retinal analogs; the conformation and environment of the protonated retinal Schiff base, studied by Raman, Fourier transform infrared, and ^{13}C solid-state NMR spectroscopies; cross-linking studies; the compensatory replacements of Glu^{113} (III:3) by Asp^{90} (II:21) or Asp^{117} (II:7); and many other data (Pogozheva et al., 1997). (Superscript residue numbers correspond to the particular receptor sequences. Numbers in parentheses indicate the helix number (Roman numerals) and the residue position in 26-residue transmembrane segments, identified by Baldwin (1993) (Arabic numerals) and shown in Fig. 1.) The "average" model of the α-bundle is also in agreement with constraints experimentally derived by site-directed mutagenesis for other GPCRs, such as the proximity of Asp^{397} (II:28) and Lys^{583} (VII:3) in the lutropin/choriogonadotropin hormone receptor (Fernandez and Puett, 1996), Asn^{87} (II:14) and Asn^{318} (VII:17) in the gonadotropin-releasing hormone receptor (Zhou et al., 1994), Asp^{120} (II:14) and Asn^{396} (VII:17) in the 5-HT$_{2A}$ receptor (Sealfon et al., 1995), Asp^{125}(III:7) and Lys^{331}(VII:4) in α_{1B}-adrenergic receptors (Porter et al., 1996), and the formation of an artificial Zn^{2+}-binding site by histidine residues incorporated in positions V:-1, V:3, and VI:27 in mutant NK-1 and κ opioid receptors (Elling et al., 1995; Thirstrup et al., 1996). The models of cationic amine receptors (Lomize et al., 1998) are consistent with accessibilities of residues from helices III, V, and VII to water-soluble probes (Javitch et al., 1995; Fu et al., 1996) and with a vast sample of site-directed mutagenesis data demonstrating, for example, the interaction of AspIII:7 with the protonated amine of ligands (Fraser et al., 1989; Javitch et al., 1995; Ho et al., 1992; Mansour et al., 1992, 1997; Porter et al., 1996; Savarese and Fraser, 1992; Strader et al., 1987, 1988; Wang et al., 1991, 1993), the involvement of SerV:6 of β-adrenoreceptors and SerV:7 of α-adrenoreceptors in H-bond formation with catechol ligands, the importance of SerV:10 for ligand binding and activation (Strader et al., 1989; Wang et al., 1991; Hwa et al., 1997), and the proximity of the indole rings of Trp^{109} (III:3) and Trp^{330} (VII:8) of the β_2-adrenoreceptor to the azido group of iodoazidopindolol, an affinity label for β-adrenergic receptors (Wong et al., 1988).

In the present paper, we discuss in detail the 3D structures of δ, μ, and κ opioid receptors calculated from the previously developed "average" model of the transmembrane domain. This is an especially interesting case for verification of the receptor models by ligand docking, because the three different opioid receptor types have a number of structurally distinct, conformationally constrained ligands, from small, rigid alkaloids to larger cyclic peptides, with well-studied structure-activity relationships (SARs). In addition, we have included in the models the tentative structures of the three extracellular loops, which were calculated by distance geometry. Although the ligand-binding pocket consists mainly of residues from the transmembrane α-bun-

TMH I

```
                  ***************************
δ    L⁴⁶ALAIAITALYSAVCAVGLLGNVLVMFGIVRYT⁷⁸
μ    M⁶⁵ITAITIMALYSIVCVCGLFGNFLVMYVIVRYT⁹⁷
κ    P⁵⁶IIPVIIMAVYSVVFVCGLVGNSLVMYVIIRYT⁸⁸
```

TMH II

```
      **    **********************
δ    A⁸³ TNIYIFNLALADALATSTLPFQSAKYLME¹¹²        EL-1 TWPFG¹¹⁷
μ    A¹⁰²TNIYIFNLALADALATSTLPFQSVNYLMG¹³¹             TWPFG¹³⁶
κ    A⁹³ TNIYIFNLALADALVTTTMPFQSTVYLMN¹²²             SWPFG¹²⁷
```

TMH III

```
                  **************************
δ    E¹¹⁸LLCKAVLSIDYYNMFTSIFTLTMMSVDRYIAVCH¹⁵²
μ    T¹³⁷ILCKIVISIDYYNMFTSIFTLCTMSVDRYIAVCH¹⁷¹
κ    D¹²⁸VLCKIVISIDYYNMFTSIFTLCTMSVDRYIAVCH¹⁶²
```

TMH IV

```
                  **************************
δ    P¹⁶²AKAKLINICIWVLASGVGVPIMVMAVT¹⁸⁹  EL-2RPRDG   AVVCMLQFPSPSW YW²⁰⁹
μ    P¹⁸¹RNAKIINVCNWILSSAIGLPVMFMATT²⁰⁸       KYRQG   SIDCTLTFSHPTW YW²²⁸
κ    P¹⁷²RNAKIINVCNWLLSSSVGVSAIVLGGT¹⁹⁹       KVREDVDVIECSLQFPDDEYSWW²²²
```

TMH V

```
                  ***************************
δ    D²¹⁰TVTKICVFLFAFVVPILIITVCY²³³
μ    E²²⁹NLVKICVFIFAFIMPVLIITVCY²⁵²
κ    E²²³LFMKICVFIFAFVIPVLIIIVCY²⁴⁶
```

TMH VI

```
                  **************************
δ    L²⁵⁶RRITRMVLVVVGAFVVCWAPIHIFVIVWTLVDI²⁸⁹    EL-3 DRRDP²⁹⁴
μ    L²⁷⁵RRITRMVLVVVAVFIVCWTPIHIYVIIKALVTI³⁰⁸          PETT³¹²
κ    L²⁶⁹RRITRLVLVVVAVFVVCWTPIHIFILVEALGST³⁰²          SHST³⁰⁶
```

TMH VII

```
                  **************************
δ    L²⁹⁵VVAALHLCIALGYANSSLNPVLYAFLD³²²
μ    F³¹³QTVSWHFCIALGYTNSCLNPVLYAFLD³⁴⁰
κ    A³⁰⁷ALSSYYFCIALGYTNSCLNPILYAFLD³³⁴
```

FIGURE 1 Sequence alignment of transmembrane helices (TMH I–TMH VII) and extracellular loops (EL-1, EL-2, EL-3) of human δ, μ, and κ receptors. Asterisks above the sequences for each helix indicate the 26-residue transmembrane segments, identified by Baldwin (1993) and used for identification of GPCR residues as the number of helix (Roman numerals):number of residue in the 26-residue fragment (Arabic numerals). For example, Asp¹²⁸ in the δ-receptor sequence is denoted as III:7. Numbering of the μ receptor is that of the rat receptor for consistency with mutagenesis data.

dle, the extracellular loops of opioid receptors have also been shown to be important for interactions with many ligands (Chen et al., 1995; Fukuda et al., 1995; Hjorth et al., 1995; Meng et al., 1995, 1996; Minami et al., 1996; Onogi et al., 1995; Pepin et al., 1997; Varga et al., 1996; Valiquette et al., 1996; Wang et al., 1994, 1995; Xue et al., 1994, 1995; Zhu et al., 1996a,b), whereas the extracellular N-terminus can be deleted in μ and κ receptors (Kong et al., 1994; Surratt et al., 1994) or exchanged between receptor subtypes (Meng et al., 1996) without affecting the ligand binding.

METHODS

The modeling described here was done in three stages: 1) distance geometry calculations of transmembrane domains of δ, μ, and κ opioid receptors from the previously determined "average" transmembrane α-bundle struc-

ture; 2) modeling of the extracellular loops of the opioid receptors; and 3) incorporation of various opioid ligands into the calculated receptor structures.

Distance geometry calculations of transmembrane α-bundles for δ, μ, and κ receptors

The transmembrane 7-α-bundles of δ, μ, and κ opioid receptors were calculated using their own specific H-bonds, while using the "average" GPCR model to restrain the spatial positions of the helices, as previously described for bovine rhodopsin (Pogozheva et al., 1997). The positions of the helices were restrained by incorporating $C^\beta \ldots C^\beta$ distances from the "average" model as the upper limits in calculations with the distance geometry program DIANA (Güntert et al., 1991). These $C^\beta \ldots C^\beta$ limits were increased by 1 Å (0.5 Å for distances of the more loosely packed helix I) to allow some relaxation of the specific receptor structures relative to the "average" model, i.e., small shifts of helices that are necessary to adopt the replacements of side chains in the "core" of the α-bundle.

To examine possible H-bonds and to determine conformers of side chains in opioid receptors, we applied an iterative distance geometry refinement approach, which we have previously described (Pogozheva et al., 1997). Each iteration of the refinement included 1) examination of the structures calculated in the previous iteration for new potential H-bonding partners (spatially proximate polar groups that did not form H-bonds in the previous iteration of the model), for correlations in sequence alignments and for structural flaws (violations of constraints, appearance of hindrances or holes produced by incorrectly packed side chains, helices that are multiply curved by contradictory constraints or are loosely packed because of insufficient constraints); 2) modification of distance and angle constraints (H-bonds and conformers of side chains) to increase the number of simultaneously formed H-bonds, and to correct discovered flaws; and 3) distance geometry calculations with the modified constraints. The analysis of calculated structures (step 1) was performed using the program ADJUST (Pogozheva et al., 1997) and the molecular modeling software QUANTA (Molecular Simulations). The constraints and the corresponding α-bundle structure evolved simultaneously during the refinement. During the refinement, conformers of most side chains were unequivocally determined. Final systems of H-bonds are shown in Table 1.

In calculations with DIANA, the α-helix geometry was restrained by backbone H-bonds (upper limits for $NH_{i...}$ $O=C_{i-4}$ distances = 1.9 Å, except those broken by Pro residues) and by dihedral angle constraints ($\varphi = -70°$ to $-50°$, $\psi = -50°$ to $-30°$). Because the program requires a single chain, the loops connecting α-helices were approximated by Gly_n fragments, with the number of Gly residues corresponding to the length of each loop in the δ-opioid receptor. In the later iterations of the calculations, glycine residues in the extracellular loops were replaced with the amino acids corresponding to the opioid receptor sequences (see below). The standard target function minimization strategy (Güntert et al., 1991) was used for calculations. The weighting factors for upper and lower distance limits and van der Waals and angle constraints initially were 1, 1, 0.6, and 20, respectively, and 1, 1, 2.0, and 5 by the final two iterations. The HisVI:20 and HisVII:4 side chains were considered to be uncharged, and all other His, Asp (including AspII:14), Glu, Lys, and Arg side chains were considered charged.

Modeling the extracellular loops

The extracellular domain of the opioid receptors consists of three loops (EL-1, EL-2, and EL-3), whose tentative structures are modeled here, and an N-terminus that was not considered (Fig. 1). It is apparent from the sequence homology of the loops among the δ, μ, and κ receptors, that essentially the same structure can be expected in the different receptor subtypes. EL-1 and EL-3 are rather short (four or five residues) (Fig. 1), whereas EL-2 is longer (20 residues in δ and μ receptors and 23 residues in the κ receptor) and can interact directly with all opioid ligands, because it partially covers the binding cavity between helices III and VII in the model of the transmembrane α-bundle. Initially, only this longer EL-2 was added to the transmembrane α-bundle for distance geometry calculations. EL-2 connects transmembrane helices (TMHs) IV and V and is attached to TMH III by a conserved disulfide bond (Watson and Arkinstall, 1994), giving this loop a U-like shape (the peptide chain comes from TMH IV toward TMH III and returns back to TMH V, as shown in Figs. 4 and 5). Both branches of the U-like EL-2 are too short to form any additional α-helices in the calculated models of the transmembrane domain, and the geometrical constraints imposed by their attachment to TMH III, IV, and V force them to adopt extended structures. This extended character of the peptide chain is also consistent with the general (i, $i + 2$) pattern of alternate polar and nonpolar side chains around the disulfide bond in amino acid sequences of opioid receptors and rhodopsins, for example. The pattern is of the form p-n-p-Cys-p-n-p-Ar, where p, n, and Ar denote polar, nonpolar, and aromatic residues, respectively. We suggest that the two extended antiparallel stretches of EL-2 near the conserved disulfide bond are paired in a β-hairpin (residues 195–203 in the δ, 214–222 in the μ, 207–215 in the κ receptor), and the two remaining fragments of EL-2, which connect the β-hairpin to helices IV and V, adopt a nonregular

structure. These connections contain Pro, Gly, and polar residues and are highly variable in families of opioid receptors and other GPCRs. The characteristic Pro^{203}-Ser^{204}-Pro^{205}-Ser^{206} sequence in the δ opioid receptor, for example, is an excellent breaker of both α-helix and β-structure. The nonregular structure of these connections can be also suggested based on insertions in this region arising in many different GPCRs, such as insertions of Ser^{220} and Val^{205}-Asp^{206} residues in the κ receptor (Fig. 1).

The hypothesized β-hairpin formation is supported by several observations. First, the β-hairpin provides the formation of many H-bonds between residues that appear and disappear in a correlated manner in amino acid sequences of opioid receptors, such as $Asp^{216}...Thr^{220}$, $Lys^{141}...Asp^{216}$, $Ser^{214}...Gln^{314}$, and $His^{223}...Glu^{310}$ (present only in μ receptors), $Glu^{118}...Gln^{201}$, $Glu^{118}...Lys^{122}$, and $Ser^{204}...Arg^{291}$ (present only in δ receptors), and $Lys^{132}...Glu^{209}$ and $Asp^{216}...His^{304}$ (present only in κ receptors). Two insertions in EL-2 of the κ receptor are also correlated: they provide simultaneous lengthening of both nonregular connections between the β-hairpin and transmembrane helices IV and V, thus allowing the β-hairpin to stay in the same spatial position. Second, the β-hairpin can readily be inserted in the cavity between helices III and VII, without the appearance of interatomic hindrances, and it forms numerous hydrophobic contacts and several hydrogen bonds with the transmembrane α-bundle. Third, the structure of the β-hairpin itself is stabilized by hydrophobic contacts of several interacting nonpolar residues (Val^{196}, Leu^{200}, and Phe^{202} in the δ receptor; Ile^{215}, Leu^{219}, and Phe^{221} in the μ receptor; or Ile^{208}, Leu^{212}, and Phe^{214} in the κ receptor; see Fig. 5). At the same time, several polar residues (Gln^{201} in δ; Asp^{216}, Thr^{218}, Thr^{221} in μ; Glu^{209}, Thr^{211}, Gln^{213} in κ receptors) are arranged on the opposite face of the β-hairpin and form H-bonds with each other and with polar residues from helix III (Glu/Thr/AspIII:-3 and LysIII:1). Fourth, the presence of several Ser and Thr residues with high β-sheet propensities in this region (positions 214, 218, 220, and 222 in the μ opioid receptor, for example) is also consistent with the hypothesized formation of the β-hairpin.

The probable conformation of the β-turn in the β-hairpin can also be readily identified. Because the β-turn consists of an odd number of residues (residues 198–200 in δ, 217–219 in μ, 210–212 in κ receptor), the only allowed standard type is the type I with a G1 β-bulge, i.e., the $\alpha_R\gamma_R\alpha_L$ motif (Sibanda and Thornton, 1991). This motif is very common in protein β-hairpins (Sibanda and Thornton, 1991) and has been shown to be independently stable in aqueous solution (deAlba et al., 1996), because, unlike the "standard" type I and II β-turns, the $\alpha_R\gamma_R\alpha_L$ turn is consistent with the direction of twist in β-structure (Richardson and Richardson, 1989). In the structure of the μ opioid receptor, this turn is further stabilized by H-bonds formed by the COO^- group of Asp^{216} with the main-chain NH group of Thr^{218}, and between the side chains of Thr^{218} and Thr^{220} (Fig. 5). The consistency of the β-hairpin with the entire system of distance constraints for the α-bundle was further verified by distance geometry calculations for δ, μ, and κ receptors (the H bonds of the β-hairpin are shown in Table 1).

After incorporation of the β-hairpin in the model, the extracellular ends of TMHs II, III, VI, and VII were extended by one to three residues (through residues II:28, III:-3, VI:3, and VII:-2), because these residues can form fragments of amphiphilic helix with nonpolar side chains facing the lipid environment. This also provides, simultaneously, many additional intra- and interhelical H-bonds and hydrophobic contacts between nonpolar side chains. The remaining extracellular loop fragments (113–117 (EL-1), 190–194 and 204–209 (EL-2), and 290–294 (EL-3) in the δ receptor; 130–136 (EL-1), 209–213 and 223–228 (EL-2), and 309–312 (EL-3) in the μ receptor; 123–127 (EL-1), 200–206 and 216–222 (EL-2), and 303–306 (EL-3) in the κ receptor) were simply considered as short, nonregular connections whose tentative structures were defined by distance geometry calculations based on the appearance of correlated H-bonded residues in the loops (such as Arg^{291}-Asp^{290} and Asp^{288}-Arg^{292}-Asp^{293}, which simultaneously appear only in EL-3 of the δ receptor), and constraints for dihedral angles φ and ψ, which fix them in the allowed areas of the Ramachandran map (the intervals of the angles were constrained similarly to that in the REDAC strategy; Güntert and Wuthrich, 1991). The final structures of the extracellular loops in all opioid receptors provide close packing of Trp and Phe residues conserved in EL-1 (positions 114

TABLE 1   H-bonds of side chains applied as distance constraints for calculation of opioid receptor models

δ receptor		μ receptor		κ receptor		Location
			Side chain to side chain			
Thr^{53}Oγ^1	Ser^{106}Hγ			Thr^{63}Oγ^1	Ser^{116}Hγ	TMHs I–II
Cys^{60}Hγ	Ser^{100}Oγ	Cys^{79}Hγ	Ser^{119}Oγ			TMHs I–II
Asn^{67}Hδ^{22}	Asp^{95}Oδ^1	Asn^{86}Hδ^{22}	Asp^{114}Oδ^1	Asn^{77}Hδ^{22}	Asp^{105}Oδ^1	TMHs I–II
Asn^{67}Oδ^1	Ser^{312}Hδ	Asn^{86}Oδ^1	Cys^{330}Hδ	Asn^{77}Oδ^1	Ser^{324}Hδ	TMHs I–VII
Thr^{78}Oγ^1	Asn^{85}Hδ^{21}	Thr^{97}Oγ^1	Asn^{104}Hδ^{21}	Thr^{88}Oγ^1	Asn^{95}Hδ^{21}	TMHs I–II
Asn^{85}Oδ^1	Tyr^{318}Hη	Asn^{104}Oδ^1	Tyr^{336}Hη	Asn^{95}Oδ^1	Tyr^{330}Hη	TMHs II–VII
Tyr^{87}Oη	Lys^{166}Hζ^1	Tyr^{106}Oη	Lys^{185}Hζ^1	Tyr^{97}Oη	Lys^{176}Hζ^1	TMHs II–IV
Tyr^{87}Hη	Asn^{169}Oδ^1	Tyr^{106}Hη	Asn^{188}Oδ^1	Tyr^{97}Hη	Asn^{179}Oδ^1	TMHs II–IV
Asn^{90}Oδ^1	Tyr^{130}Hη	Asn^{109}Oδ^1	Tyr^{149}Hη	Asn^{100}Oδ^1	Tyr^{140}Hη	TMHs II–III
Asn^{90}Hδ^{21}	Thr^{138}Oγ^1	Asn^{109}Hδ^{21}	Thr^{157}Oγ^1	Asn^{100}Hδ^{21}	Thr^{148}Oγ^1	TMHs II–III
Asn^{90}Oδ^1	Trp^{173}Hε^1	Asn^{109}Oδ^1	Trp^{192}Hε^1	Asn^{100}Oδ^1	Trp^{183}Hε^1	TMHs II–IV
Asp^{95}Oδ^2	Asn^{131}Hδ^{22}	Asp^{114}Oδ^2	Asn^{150}Hδ^{22}	Asp^{105}Oδ^2	Asn^{141}Hδ^{22}	TMHs II–III
Asp^{95}Oδ^2	Asn^{314}Oδ^1*	Asp^{114}Oδ^2	Asn^{332}Oδ^1*	Asp^{105}Oδ^2	Asn^{326}Oδ^1*	TMHs II–VII
Thr^{99}Hγ^1	Ser^{312}Oγ	Thr^{118}Hγ^1	Cys^{330}Sγ	Thr^{109}Hγ^1	Ser^{324}Oγ	TMHs II–VII
Gln^{105}Hε^{22}	Asp^{128}Oδ^1	Gln^{124}Hε^{22}	Asp^{147}Oδ^1	Gln^{115}Hε^{22}	Asp^{138}Oδ^1	TMHs II–III
Gln^{105}Oε^1	His^{301}Hε^2	Gln^{124}Oε^1	His^{319}Hε^2			TMHs II–VII
Ser^{106}Hγ	His^{301}Nδ^1	Ser^{125}Hγ	His^{319}Nδ^1			TMHs II–VII
		Tyr^{128}Oη	Thr^{312}Hγ^1			TMHs II–VII
				Tyr^{119}Oη	Thr^{306}Hγ^1	TMHs II–VII
Glu^{118}Oε^1	Lys^{122}Nζ					TMHs III–III
		Thr^{137}Hγ^1	Asp^{216}Oδ^1			TMHs III–EL-2
Glu^{118}Oε^2	Gln^{201}Hε^{22}			Asp^{128}Oδ^1	Gln^{213}Hε^{22}	TMHs III–EL-2
		Lys^{141}Nζ	Asp^{216}Oδ^2	Lys^{132}Nζ	Glu^{209}Oε^1	TMHs III–EL-2
Asp^{128}Oδ^2	Tyr^{308}Hη	Asp^{147}Oδ^2	Tyr^{328}Hη	Asp^{138}Oδ^2	Tyr^{323}Hη	TMHs II–VII
Asn^{131}Oδ^1	Ser^{311}Hγ	Asn^{150}Oδ^1	Ser^{329}Hγ	Asn^{141}Oδ^1	Ser^{311}Hγ	TMHs III–VII
Thr^{134}Oγ^1	Ser^{177}Hγ*	Thr^{153}Oγ^1	Ser^{196}Hγ*	Thr^{144}Oγ^1	Ser^{187}Hγ*	TMHs III–IV
Ser^{135}Hγ	Asn^{314}Oδ^1	Ser^{154}Hγ	Asn^{332}Oδ^1	Ser^{145}Hγ	Asn^{326}Oδ^1	TMHs III–VII
		Thr^{160}Hγ^1	Asn^{191}Oδ^1			TMHs III–IV
Asp^{145}Oδ^1	Arg^{146}Hη^{12}	Asp^{164}Oδ^1	Arg^{165}Hη^{12}	Asp^{155}Oδ^1	Arg^{156}Hη^{12}	TMHs III–III
Asp^{145}Oδ^2	Lys^{164}Hζ^1*	Asp^{164}Oδ^2	Asn^{183}Hδ^{22}*	Asp^{155}Oδ^2	Lys^{174}Hζ^1*	TMHs III–IV
Asp^{145}Oδ^2	Lys^{166}Hζ^2	Asp^{164}Oδ^2	Lys^{185}Hζ^2	Asp^{155}Oδ^2	Lys^{176}Hζ^2	TMHs III–IV
				Lys^{200}Nζ	Asp^{204}Oδ^1	EL-2–EL-2
Arg^{190}Nη^1	Ser^{206}Oγ					EL-2–EL-2
				Arg^{202}Hη^{12}	Asp^{217}Oδ^1	EL-2–EL-2
				Arg^{202}Hη^{11}	Glu^{218}Oε^1	EL-2–EL-2
		Gln^{212}Hε^{22}	Asp^{216}Oδ^1			EL-2–EL-2
		Gln^{212}Oε^1	Ser^{222}Oγ			EL-2–EL-2
				Asp^{204}Oδ^2	Ser^{220}Hγ	EL-2–EL-2
				Asp^{206}Oδ^2	His^{304}Hδ^1	EL-2–EL-3
		Ser^{214}Oγ	Gln^{314}Hδ^{22}			EL-2–TMH VII
		Thr^{218}Oγ^1	Thr^{220}Oγ^1	Ser^{211}Oγ	Gln^{213}Hε^{21}	EL-2–EL-2
Ser^{204}Oγ	Arg^{291}Hε	His^{223}Hδ^1	Glu^{310}Oε^1	Asp^{216}Oδ^1	His^{304}Hδ^1	EL-2–EL-3
		His^{223}Hδ^1	Gln^{314}Oε^1			EL-2–TMH VII
Tyr^{208}Hη	Met^{186}Sδ	Tyr^{227}Hη	Met^{205}Sδ	Trp^{221}Hε^2	Met^{216}Sδ	EL-2–TMH IV
Asp^{210}Oδ^1	Lys^{214}Hζ^1	Glu^{229}Oε^1	Lys^{233}Hζ^1	Asp^{223}Oδ^1	Lys^{227}Hζ^1	TMHs V–V
		Asn^{230}Oδ^1	Lys^{233}Hζ^2			TMHs V–V
Tyr^{233}Oη	Arg^{261}Hε	Tyr^{252}Oη	Arg^{280}Hε	Tyr^{246}Oη	Arg^{274}Hε	TMHs V–VI
		Tyr^{299}Hη	Ser^{317}Oγ			TMHs VI–VII
		Lys^{303}Hζ^2	Ser^{317}Oγ			TMHs VI–VII
Asp^{288}Oδ^2	Arg^{292}Hε					TMHs VI–EL-3
Asp^{290}Oδ^2	Arg^{291}Nη^2					EL-3–EL-3
Arg^{292}Nη^1	Asp^{293}Oδ^2					EL-3–EL-3
Arg^{292}Nη^2	Asp^{293}Oδ^1					EL-3–EL-3
Asn^{310}Oδ^1	Asn^{314}Hδ^{22}	Asn^{328}Oδ^1	Asn^{332}Hδ^{22}	Asn^{322}Oδ^1	Asn^{326}Hδ^{22}	TMHs VI–VII
			Side chain to main chain			
Tyr^{56}Hη	Thr^{99}O	Tyr^{75}Hη	Thr^{118}O	Tyr^{66}Hη	Thr^{109}O	TMHs I–II
Asn^{85}Hδ^{22}	Lys^{81}O	Asn^{104}Hδ^{22}	Lys^{100}O	Asn^{95}Hδ^{22}	Lys^{91}O	TMHs II–IL1
Tyr^{87}Oη	Ala^{165}O*	Tyr^{106}Oη	Ala^{184}O*	Tyr^{97}Oη	Ala^{175}O*	TMHs II–IV
Lys^{108}Nζ	Trp^{114}O					TMH II–EL1

H-bonds between residues in corresponding positions in the sequences of δ, μ, and κ receptors are shown in the same row. Upper distance constraints were 1.9 Å for H. . .O, 2.9 Å for O. . .O and N. . .O, and 2.6 Å for H. . .S bonds. In addition, 15, 18, and 22 H-bonds of threonine and serine side chains with $i - 4$ backbone carbonyls are also included for δ, μ, and κ receptors, respectively.

*Distances increased by 0.3 Å.

TABLE 1 Continued

δ receptor		μ receptor		κ receptor		Location
$Lys^{108}N\zeta$	$Cys^{198}O$					TMH II–EL-2
		$Asn^{127}H\delta^{22}$	$Gly^{136}O$			TMH II–EL-1
$Tyr^{109}H\eta$	$Pro^{294}O$	$Tyr^{128}H\eta$	$Thr^{312}O$	$Tyr^{119}H\eta$	$Thr^{306}O$	TMH II–EL-3
$Thr^{113}H\gamma^1$	$Met^{111}O$	$Thr^{132}H\gamma^1$	$Met^{130}O$	$Thr^{123}H\gamma^1$	$Met^{121}O$	TMH II–EL-1
				$Asp^{128}H\delta^1$	$Ser^{211}HN$	TMH III–EL-2
				$Asp^{128}H\delta^1$	$Asp^{128}HN$	TMHs III–III
$Arg^{190}H\varepsilon$	$Arg^{192}O$	$Lys^{209}N\zeta$	$Arg^{211}O$	$Lys^{200}N\zeta$	$Arg^{192}O$	EL-2–EL-2
		$Gln^{212}O\varepsilon^1$	$Gly^{213}HN$	$Glu^{203}O\varepsilon^1$	$Asp^{204}HN$	EL-2–EL-2
		$Gln^{212}O\varepsilon^1$	$Ser^{214}HN$	$Glu^{203}O\varepsilon^1$	$Val^{205}HN$	EL-2–EL-2
				$Asp^{203}O\delta^2$	$Trp^{221}HN$	EL-2–EL-2
				$Asp^{216}O\delta^2$	$Ser^{220}HN$	EL-2–EL-2
		$Asp^{216}O\delta^1$	$Thr^{218}HN$			EL-2–EL-2
$Ser^{204}H\gamma$	$Asp^{290}O$					EL-2–TMH VII
$Ser^{206}H\gamma$	$Arg^{192}O$					EL-2–EL-2
$Trp^{207}H\varepsilon^1$	$Leu^{286}O$	$Trp^{226}H\varepsilon^1$	$Leu^{305}O$	$Tyr^{219}H\eta$	$Leu^{299}O$	EL-2–TMH VII
$Asp^{288}O\delta^1$	$Val^{296}HN$					TMHs VI–VII
$Arg^{291}N\varepsilon$	$Ser^{204}O$					EL-3–EL-2
$Asn^{310}H\delta^{22}$	$Val^{266}O$	$Asn^{328}H\delta^{22}$	$Val^{285}O$	$Asn^{322}H\delta^{22}$	$Val^{279}O$	TMHs VII–VI

and 116 in δ, 133 and 135 in μ, and 124 and 126 in κ receptors) and the orientation of most tryptophan, tyrosine, and phenylalanine side chains in the loops toward the lipid-water interface, where they can interact with lipid headgroups, as is characteristic for membrane proteins (Deisenhofer and Michel, 1991; Schultz, 1992; Grigorieff et al., 1996).

Final calculations of the transmembrane domains, including the three extracellular loops, were made using 64, 69, and 70 side-chain H-bonding constraints for δ, μ, and κ receptors, respectively (Table 1); constraints for dihedral angles of the main chain in the loops and for all side chains of the transmembrane α-bundle; $C^\beta \ldots C^\beta$ distance constraints taken from the "average" model; and restraints on the geometry of the TMHs, as described above. The constraints also included backbone H-bonds in the β-hairpin of the EL-2 fragment (residues 195–203 in δ, 214–222 in μ, 207–215 in κ receptor) and a conserved disulfide bond connecting this β-hairpin to TMH III. Totals of 877, 896, and 884 angle constraints and 691, 690, and 651 distance constraints were used for calculations of δ, μ, and κ receptors, respectively.

The calculations with DIANA yielded well-defined sets of structures for each (δ, μ, and κ) opioid receptor (pairwise r.m.s.d. of 212 TMH C^α atoms was <0.7 Å for the 10 structures of each receptor with the lowest target function). The r.m.s.d. between C^α atoms of TMHs of different (δ, μ, and κ) receptors was larger (~0.9 Å). All backbone angles of the models are within the allowed regions of the Ramachandran map, and all side chains have standard χ^1-χ^4 conformers, as is automatically provided by the dihedral angle constraints (violations of the individual angle constraints were <10°). A few violations of van der Waals constraints of ~0.5 Å were present near Pro residues in α-helices; no violations of H-bond distances greater than 0.6 Å were found. The structures of receptors with the lowest target function were selected for ligand docking and energy minimization.

Ligand docking

All opioid ligands were inserted manually into the binding pockets, using the Molecular Modeling module of QUANTA to move the ligands and control hindrances and receptor-ligand H-bonds. The docking was simplified by using only rigid or conformationally constrained ligands (Fig. 2 and Tables 2 and 3) whose structures have been solved by x-ray crystallography (Bye, 1976; Klein et al., 1987; Urbanczyk-Lipkowska and Etter, 1987; Verlinde et al., 1984; Calderon et al., 1997; Doi et al., 1990; Flippen-Anderson and George, 1994; Griffin et al., 1986; Lomize et al., 1994; Collins et al., 1996) or NMR spectroscopy (Mosberg and Sobczyk-Kojiro, 1991; Collins et al., 1996). The procedure of manual ligand docking is similar to assembling a jigsaw puzzle that consists of two semirigid pieces; however, three circumstances complicated the process. First, because most

of the ligands are not completely rigid, it was necessary to consider several possible conformers of their flexible elements, such as the *N*-cyclopropylmethyl group in morphine, the *N*-phenethyl group in fentanyl, or Tyr[1] in cyclic opioid peptides. Second, in a few cases, described in the Results, it was necessary to adjust conformers of several receptor side chains in the binding pocket, which were not unequivocally defined by distance geometry calculations. Third, because the DIANA-generated receptor structures were not completely identical (although the r.m.s.d of C^α atoms was low: ~0.7 Å), the ligand docking was performed with two or three structures with the lowest target function.

The receptor-ligand H-bonds and ion pairs served as important attachment points for ligand docking. Two such attachment points are the carboxyl and imidazole groups of AspIII:7 and HisVI:20, respectively, the only polar groups situated at the bottom of the binding pocket in all three calculated opioid receptor models (δ, μ, and κ). The importance of the AspIII:7 and HisVI:20 residues for binding opioid ligands has been clearly demonstrated by mutagenesis (Befort et al., 1996b; Mansour et al., 1997; Surratt et al., 1994). In the receptor models, these carboxyl and imidazole groups are arranged in such a way that they can interact simultaneously with the N^+ and OH groups, respectively, of the Tyr[1] or tyramine group present in most opioid ligands. Importantly, all surrounding side chains in the bottom of the binding pockets (IleV:4, IleVI:19, CysVII:6, IleVII:7) can be tightly packed (arranged without hindrances or holes) with the tyramine fragment of the ligands. It should be mentioned that, even without consideration of receptor-ligand H-bonds, the largest ligands, such as norBNI and cyclic peptides, can be inserted in the binding pockets without hindrances in only one way, because they occupy nearly all available space within the pockets, and any shift of the ligands would produce significant overlaps with surrounding receptor atoms. However, for some smaller ligands, the mode (or modes) of docking can be determined only if key attachment points of the interacting molecules (H-bonds or ionic interactions) are assumed.

Technically, docking of most ligands was performed in two steps. First, the tyramine fragment of each ligand was placed in the bottom of the binding pocket to form H-bonds with AspIII:7 and HisVI:20, while the rest of the ligand molecule was oriented toward the extracellular surface. Then the spatial position of the ligand molecule and the conformation of its flexible elements, which are connected to the tyramine fragment, were adjusted to exclude all hindrances with receptor atoms and to form additional H-bonds and hydrophobic contacts in the binding pocket. For example, the cyclic peptides considered (Table 3) have rigid, well-defined structures of their cycles (D-Cys-Phe-D-Pen and D-Pen-Ala-Phe-D-Pen), but have a considerably more flexible exocyclic Tyr[1] residue and side chain of Phe[3] (Deschamps et al., 1996; Lomize et al., 1996). Only structures of the
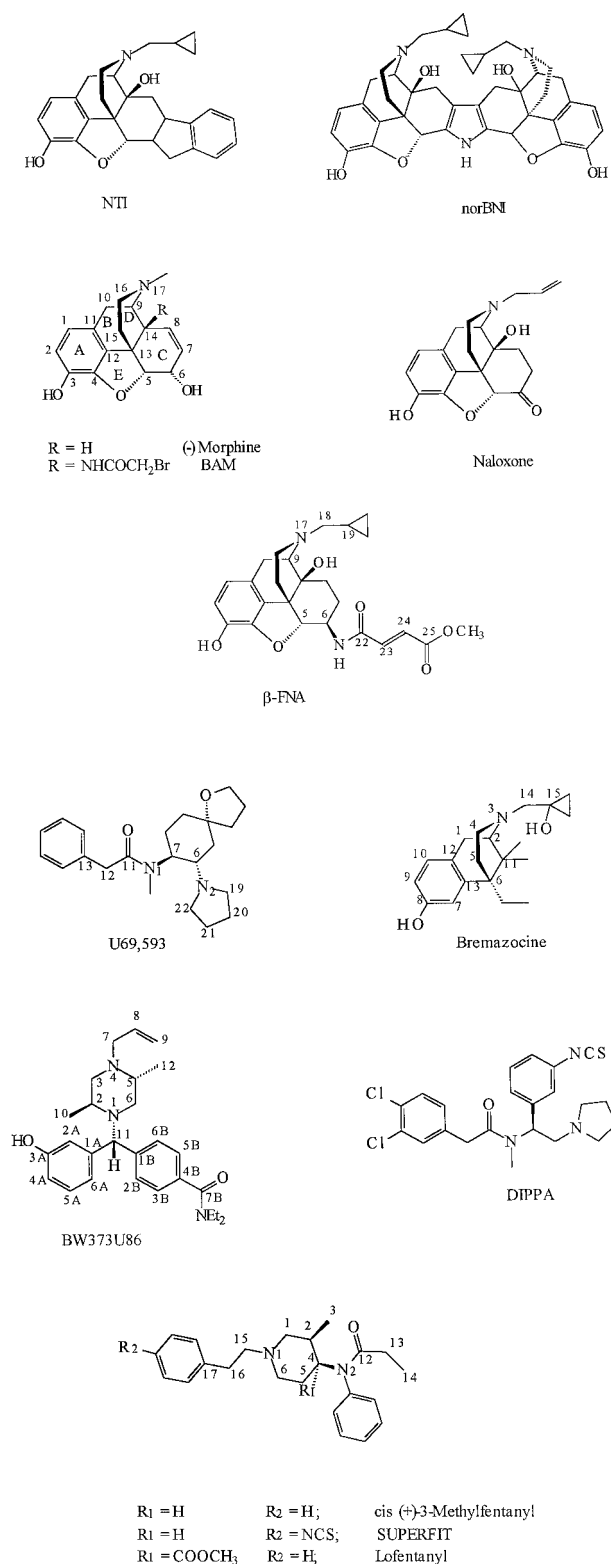
FIGURE 2   Structures of nonpeptide opioid ligands.

cycles that were determined by x-ray crystallography (Lomize et al., 1994; Flippen-Andersen et al., 1994; Collins et al., 1996) were examined here. The structure of the rigid cycle (D-Cys-Δ^EPhe-D-Pen) for the μ-selective agonist JH-42 was considered to be close to the crystal structure of JOM-13 cycle on the basis of theoretical conformational analysis (Mosberg et al.,

1996). However, during step 2 of the docking procedure, the ψ angle of Tyr^1, the φ angle of the second residue, and the χ^1 angles of the Phe$^{3(4)}$ and Tyr^1 side chains in these peptides were adjusted to allow the formation of additional H-bonds and to exclude steric hindrances with the receptor. Some details of the adjustment for the peptides and other opioid ligands are described in the Results and Discussion. It should be stressed that the bound conformations obtained for all ligands were identical or very close to the crystal structures, both geometrically (Tables 2 and 3) and energetically (the energy differences between crystal and bound conformations were 0.5–2.0 kcal/mol after energy minimization of the ligands with the CHARMm force field (Brooks et al., 1983; Momany and Rone, 1992), using a dielectric constant $\epsilon = 10$ and the adopted-basis Newton-Raphson method). Conformational analyses of peptides from the JOM-13 and [D-Pen^2,D-Pen^5]enkephalin (DPDPE) series have been discussed elsewhere (Lomize et al., 1994, 1996; Mosberg et al., 1994a,b, 1996). The proposed docking modes were compared with available SAR, cross-linking, and mutagenesis data, as described in detail in the Results and Discussion for 16 opioid ligands.

After manual docking of the ligands with the Molecular Modeling module of QUANTA, the steric overlaps between ligand and receptor atoms did not exceed 0.5 Å. All remaining hindrances were removed during 35 subsequent iterations of unconstrained minimization of the complexes with the CHARMm force field (Brooks et al., 1983; Momany and Rone, 1992), using a dielectric constant $\epsilon = 3$ and the adopted-basis Newton-Raphson method. Initial approximations that yielded energies greater than -2000 kcal/mol after 35 minimization steps were rejected, because this demonstrated residual hindrances or distorted geometry of ligands or receptor. The final energies of accepted receptor-ligand complexes ranged from -2803 to -2176 kcal/mol, and the structures of these complexes were not altered after short-term minimization: the r.m.s.d. between atoms of ligand and of receptor binding site residues from the initial and minimized structures were <0.1 Å.

RESULTS AND DISCUSSION

Models of δ, μ, and κ opioid receptors

The calculated δ, μ, and κ opioid receptor models are nearly identical within the transmembrane domain (r.m.s.d. of 212 common C$^\alpha$ atoms of the TMHs are ~0.9 Å); however, small differences are observed in the extracellular loops (Fig. 3) because of unequal numbers of residues among the receptors (Fig. 1). All opioid receptor models have a ligand-binding cavity that is partially covered by the extracellular loops (Fig. 4). The loops create an almost continuous surface, with the β-hairpin formed by EL-2 in the middle (Fig. 5), surrounded by the smaller, nonregular EL-1 and EL-3. This region is represented in 3D EM maps of frog and bovine rhodopsins by a considerable amount of electron density that does not contain α-helices (Unger et al., 1997).

The calculated opioid receptors structures have several clusters of polar side chains that form extensive networks of interhelical hydrogen bonds (Fig. 6 and Table 1). Four such clusters consist of a "core set" of polar residues that are conserved throughout most GPCRs, augmented by more variable, peripheral polar residues that are connected to the central "core" by H-bonds (Pogozheva et al., 1997). The large, polar cluster I consists of conserved AsnI:18, AspII:14, SerIII:14, AsnVII:13, SerVII:14, and AsnVII:17 residues (Asn^{86}, Asp^{114}, Ser^{154}, Asn^{328}, Ser^{329}, and Asn^{332} in the μ receptor) and is supplemented, in opioid receptors, by the more variable TyrI:7, ThrII:18, AsnIII:10, Ser/Cys-

TABLE 2   Torsion angles (degrees) of nonpeptide opiates in the models of receptor-ligand complexes and in published crystal structures of the ligands*

Compound	Receptor	Torsion angle	Receptor bound conformation			Crystal structure	Reference
BW373U86	δ	C_3-N_4-C_7-C_8	-48			-57	Calderon et al. (1997)*
		N_4-C_7-C_8-C_9	151			-149	
		C_2-N_1-C_{11}-C_{1A}	64			67	
		N_1-C_{11}-C_{1A}-C_{2A}	-98			-99	
		N_1-C_{11}-C_{1B}-C_{2B}	-152			-165	
		C_{3B}-C_{6B}-C_{7B}-N_{1B}	116			124	
			C				
SUPERFIT	δ	C_1-N_1-C_{15}-C_{16}	83			-169	Flippen-Anderson and
		N_1-C_{15}-C_{16}-C_{17}	-74			-175	George (1994)
		C_2-C_4-N_2-C_{12}	-88			-77	
		N_2-C_{12}-C_{13}-C_{14}	-57			-61	
			A	B	C		
cis-(+)-3-Methyl-fentanyl	μ	C_1-N_1-C_{15}-C_{16}	-169	-170	86	-169	Flippen-Anderson and
		N_1-C_{15}-C_{16}-C_{17}	-161	-29	-78	-175	George (1994)
		C_2-C_4-N_2-C_{12}	-77	-96	-78	-77	
		N_2-C_{12}-C_{13}-C_{14}	-83	-121	-158	-61	
β-FNA	μ	C_9-N_{17}-C_{18}-C_{19}	-179			176	Griffen et al. (1986)
		C_5-C_6-N_6-C_{21}	137			129	
		N_6-C_{21}-C_{22}-C_{23}	179			-163	
U69,593	κ	C_7-C_6-N_2-C_{19}	77			68	Doi et al. (1990)
		C_6-C_7-N_1-C_{11}	-110			-121	
		N_1-C_{11}-C_{12}-C_{13}	-100			-94	

Compounds and torsion angles are shown in Fig. 2.

*Crystal structure of the closely related 3-F analog.

VII:15 (Tyr[75], Thr[118], Asn[150], and Cys[330] in the μ receptor). Cluster I contains a cavity that can be filled by water or by a sodium ion coordinated with oxygens of the AspII:14, AsnIII:10, SerIII:14, SerVII:14, and AsnVI:17 side chains.

Cluster II is formed around the conserved AsnII:9-TrpIV:11 pair by TyrIII:9, ThrIII:13, ThrIII:17, and SerIV:15 (Asn[108]-Trp[192] pair and residues Tyr[149], Thr[153], Thr[157], and Ser[196] in the μ receptor). Cluster III consists of the con-

TABLE 3   Torsion angles of two small cyclic opioid peptides, JOM-13 (Tyr-c[D-Cys-Phe-D-Pen]) and [L-Ala³]DPDPE (Tyr-c[D-Pen-Ala-Phe-D-Pen]), in the models of δ opioid receptor-ligand complexes and in published crystal structures of the peptides

Residue	Torsion angle	JOM-13		[L-Ala³]DPDPE	
		In the model	In crystal*	In the model	In crystal#
Tyr[1]	ψ	137	102	94	120
	χ^1	176	-171	-152	-173
D-Cys/Pen[2]	φ	71	67	87	75
	ψ	25	18	12	17
	χ^1	-60	-51	-56	-60
	χ^2	-143	-141	-169	-174
	χ^3 (SS)	90	89	102	115
Ala[3]	φ	—	—	-84	-88
	ψ	—	—	-50	-42
Phe[3(4)]	φ	-76	-84	-119	-125
	ψ	-23	-15	-8	-28
	χ^1	-63	-70	-46	-56
D-Pen[4(5)]	φ	131	133	96	124
	χ^1	-77	-76	-98	-86
	χ^2	47	50	70	66

*From Lomize et al. (1994). The torsion angles within the 11-membered ring correspond to molecule A, and torsion angles for the exocyclic Tyr residue and Phe side chain correspond to molecule B (two independent molecules were present in the unit cell).

#From Collins et al. (1996). The torsion angles are for the second of four independent molecules in the crystal unit cell (conformation of the first molecule in the unit cell differs by ~15°, for several angles, from molecules 2, 3, and 4, which are nearly identical).
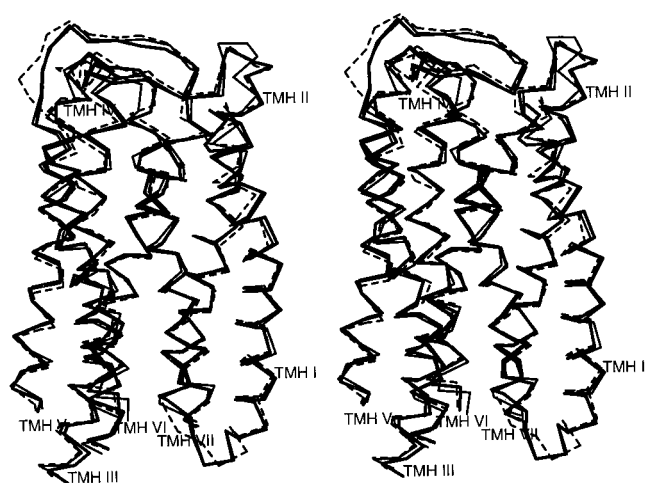
FIGURE 3   Superposition of structures of DIANA-calculated δ (*bold line*), μ (*thin line*), and κ (*dashed line*) receptors (stereo view). The r.m.s.d. between 212 C^α atoms of transmembrane helices of δ and μ, δ and κ, and μ and κ receptors are 0.74, 0.80, and 0.90 Å, respectively.

served AsnII:4 and TyrVII:21 (Asn[104] and Tyr[336] in the μ receptor) and the more variable ThrI:28 and AspVII:25 (Thr[97] and Asp[340] in the μ receptor), and cluster IV consists of the conserved triad AspIII:24-ArgIII:25-TyrIII:25 (Asp[164], Arg[165], Tyr[166] in the μ receptor) at the C-terminus of TMH III, TyrV:22, and ArgVI:3 (Tyr[252], Arg[280] in the μ receptor) from the ends of helices V and VI and the more variable TyrII:6, ThrIII:20, SerIII:22, Lys/AsnIV:2, LysIV:4, AsnIV:7, and Asn IV:10 (Tyr[106], Thr[160], Ser[162], Asn[183], Lys[185], Asn[188], Asn[191] in the μ receptor). Clusters I and II are situated in the middle of the transmembrane domain, and III and IV are close to the intracellular surface. These clusters are present in most GPCRs because they contain many conserved polar residues. The opposite, extracellular surface of the α-bundle, which includes the binding pocket, forms several smaller "variable" polar clusters that are specific for different subfamilies of GPCRs. Some of the subfamily-specific clusters are present in all opioid receptors (GlnII:24-TyrII:28-AspIII:7-TyrVII:11-His/TyrVII:4 and TyrIII:8-Asp/GluV:-1-LysV:3 (Gln[124]-Tyr[128]-Asp[147]-His[310]-Tyr[316] and Tyr[148]-Glu[229]-Lys[233] in the μ receptor)), whereas others are found only in μ (Thr[137]-Lys[140]-Asp[216]-Thr[218]-Thr[220], Ser[214]-Asn[230]-Gln[314]-His[223]-Glu[310], and Tyr[299]-Lys[303]-Ser[317]; Figs. 5 and 6), δ (Glu[118]-Lys[122]-Gln[201], Ser[204]-Arg[291]-Asp[290], and Asp[288]-Arg[292]-Asp[293]), or κ (Asp[128]-Lys[132]-Glu[209]-Gln[213], Lys[200]-Arg[202]-Asp[204]-Asp[217]-Glu[218]-Ser[220], Glu[297]-Thr[302]-Ser[311]-Tyr[312], and Asp[206]-Asp[216]-His[304]; Table 1) subtypes. Extracellular loops 2 and 3 are connected by a His[223]. . . Glu[310] H-bond in the μ receptor (Asp[216]. . . His[304] and Ser[204]. . . Arg[291] in κ and δ receptors, respectively). This H-bond is probably structurally important, because alkylation of His[223] by *N*-ethylmaleimide in the μ receptor reduces the binding affinity of several opioid ligands (Shahrestanifar et al., 1996).

The positions and tilts of the helices of the transmembrane domain of our models differ from all previously

published models of opioid receptors (Alkorta and Loew, 1996; Befort et al., 1996b; Cappelli et al., 1996; Knapp et al., 1995; Habibi-Nezhad et al., 1996; Metzger et al., 1996) and other GPCRs that have been deposited in the PDB (Bernstein et al., 1977), GPCRDB (http://swift.embl-heidelberg.de/7tm/) (Oliveira et al., 1993), and CORD (http://www.opioid.umn.edu) databases. The largest deviations of our δ opioid receptor structure (r.m.s.d. of C^α atoms in the range of 4.2–6.5 Å) are observed when compared with the earliest GPCR models, which were constructed from non-homologous bacteriorhodopsin structures, or by using 2D (projection) EM maps of rhodopsin and a few supplementary experimental constraints. The incorporation of geometric constraints derived from 3D EM maps of rhodopsins (Herzyk and Hubbard, 1995) leads to a model with a smaller (3.9 Å) deviation from our structure. Recently an improved approximation of the transmembrane domain structure has been obtained by the direct fit of two kinked and five straight helices to the 3D EM map of frog rhodopsin (Baldwin et al., 1997). This model has the lowest r.m.s.d (3.3 Å for 179 common C^α-atoms; Fig. 7) when compared with our structures of the transmembrane domain of the δ opioid receptor or bovine rhodopsin. The 3.3-Å r.m.s.d. between this model and our model of δ opioid receptor originates from the outward shifts of helices II and V, the shift of the C-terminus of helix III, and from an almost one-turn shift of helices V and VI in the direction perpendicular to the membrane plane in the model of Baldwin et al. (1997). As a result, and as discussed by the authors themselves, the model of Baldwin et al. (1997) contradicts some experimental data, such as the observed formation of a Zn^{2+} binding cluster in positions V:-1 and VI:27 and in positions V:3 and VI:27 (Elling et al., 1995; Thirstrup et al., 1996); formation of H-bonds between residues III:7, V:3, V:6, V:7 and catecholamine ligands (Strader et al., 1987, 1988, 1989; Wess et al., 1991); interaction of Asp II:14 and Asn VII:17 (Zhou et al., 1994; Sealfon et al., 1995); and the contact of Gly III:11 and Phe VI:12 in rhodopsin (Han et al., 1996a,b). All of these experimental data are simultaneously satisfied in our models (the models are compared in more detail by Lomize et al., 1998).

Our previously developed model of rhodopsin considered the possible rotations of several functionally important, conserved side chains (GluIII:24, TyrV:22, TrpVI:16, LysVII:11, and TyrVII:21) that can participate in alternative systems of H-bonds, depending on their possible χ^1 conformers ($\chi^1 \approx -60°$ or $180°$) (Pogozheva et al., 1997). Analysis of physicochemical data for rhodopsin indicates that conformational rearrangements of these side chains could take place during photoactivation of rhodopsin. In opioid receptors, only *gauche*[+] ($\chi^1 \approx -60°$) rotamers of the corresponding TrpVI:16 and TyrVII:11 and the *trans* ($\chi^1 \approx 180°$) rotamer of AspIII:24 have H-bond partners and/or lack hindrances with surrounding atoms. Therefore rotations of the side chains of these residues are unlikely. On the other hand, rotations of the TyrV:22 and TyrVII:21 side chains are possible, because there is space in the models for

FIGURE 4 Cartoon representation of transmembrane helices and extracellular loops of δ-opioid receptors with JOM-13, side view and top view from the extracellular surface. Helical fragments are purple, loop fragments are white, the β-turn is orange, the disulfide bridge between helix III and EL-2 (residues Cys[121]–Cys[198]) is yellow, and JOM-13 is green.
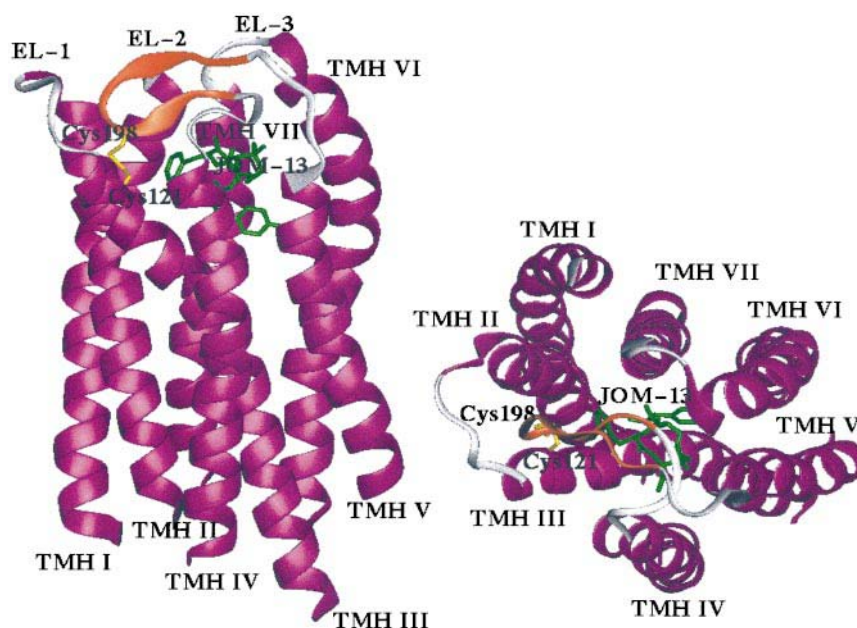
both rotamers. Consequently, distance geometry calculations were performed with two different orientations of the TyrV:22 and TyrVII:21 side chains. The two sets of structures obtained were almost identical (r.m.s.d. ∼0.7 Å). Hence the precision of our calculations is insufficient to discriminate the active and inactive conformations of opioid receptors or to reproduce the shifts of transmembrane helices that probably accompany activation of GPCRs (Sakmar and Fahmy, 1995; Farrens et al., 1996; Sheikh et al., 1996; Shieh et al., 1997). Consequently, we incorporated opioid agonists and antagonists into the same receptor structures, calculated with *trans* rotamers of the TyrV:22 and TyrVII:21 side chains, earlier assigned to the active conformation of rhodopsin.

Ligand binding

The calculated δ, μ, and κ receptor structures have deep binding cavities, situated in the extracellular side of the transmembrane domain between helices III, IV, V, VI, and VII. These cavities are partially covered by the extracellular loops and, especially, by the central β-hairpin connecting TMHs IV and V (Fig. 4). The binding pockets consist of an inner interhelical "conserved region" that is identical in δ, μ, and κ opioid receptors (GlnII:24, TyrII:28, CysIII:0, LysIII:1, ValIII:3, AspIII:7, TyrIII:8, MetIII:11, LysV:3, IleV:4, PheV:7, TrpVI:16, IleVI:19, HisVI:20, CysVII:6, IleVII:7, and TyrVII:11, and a conserved Cys in EL-2) and a peripheral "variable region" that consists of residues from the ends of TMHs (positions III:-3, III:4, V:-1, V:0, VI:23, VI:26, VI:27, VI:31, VII:-1, VII:0, VII:3, VII:4) and from the extracellular loops (for example, positions 193, 194, 195, 196, 197, 291, 293 in EL-2 and EL-3 of the δ receptor). The majority of residues in the binding pocket have fixed side-chain orientations. However, several residues can have different rotamers to accommodate either bound peptides or alkaloids: AspIII:7 has $\chi^1 \approx -60°$ for peptide ligands and $\chi^1 \approx 180°$ for alkaloid ligands; HisVI:20 has $\chi^2 \approx 120°$ or $-40°$ when interacting with peptide or alkaloid ligands, respectively; LysV:3 assumes a χ^3 angle of $180°$ or $-60°$,

FIGURE 5 Proposed structure of the β-hairpin in EL-2 of the μ opioid receptor with proximal H-bonded polar residues from helices III and VII and from EL-3 and conserved disulfide bond between Cys[140](III:0) and Cys[217](EL-2). H-bonds are indicated by the dashed line.
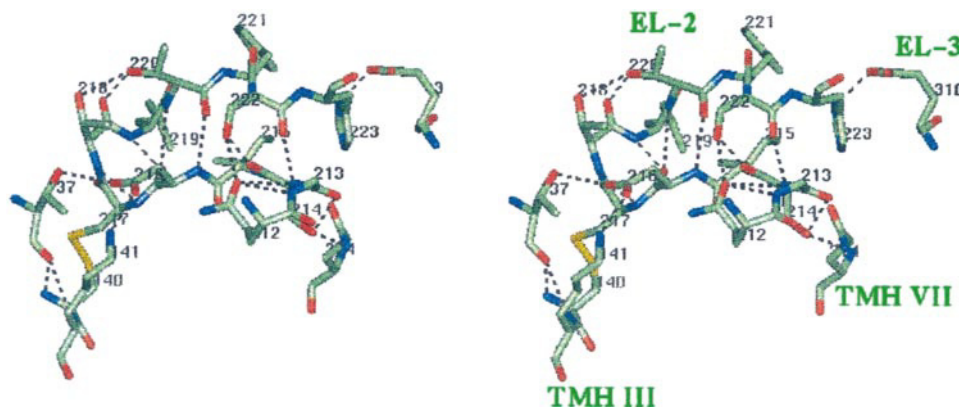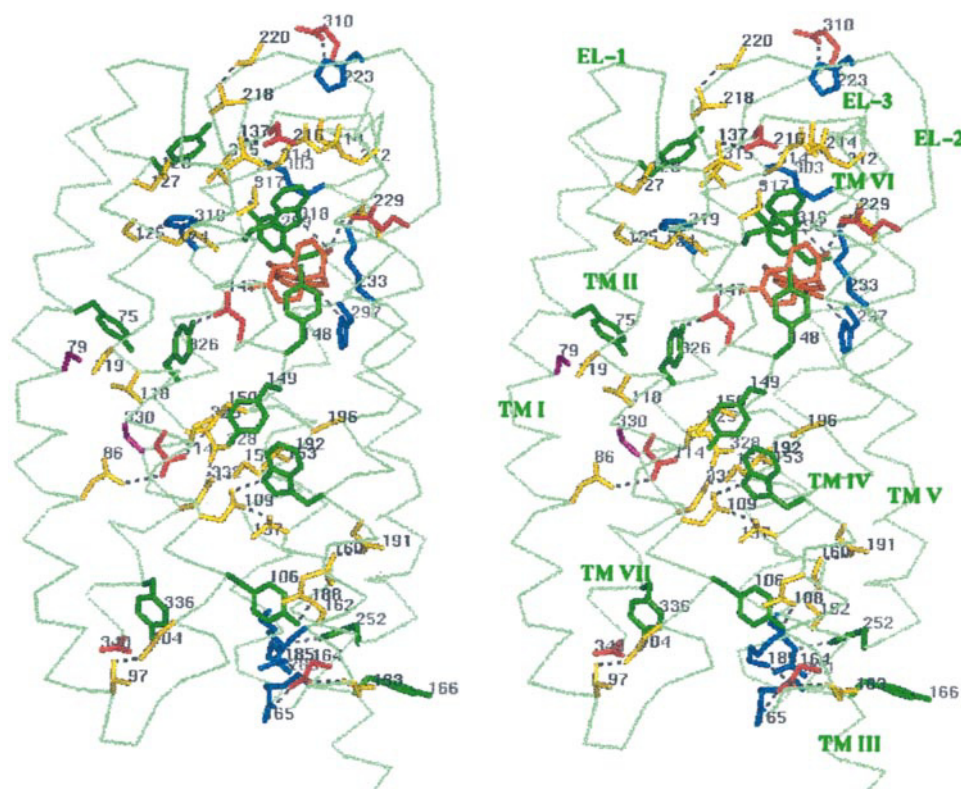
FIGURE 6   H-bond network of the μ opioid receptor (stereo view). Colors of residues depicted: green, Tyr, Trp; red, Asp, Glu; blue, His, Lys; yellow, Ser, Thr, Asn, Gln. The receptor is shown with morphine (*purple*) in the binding site. H-bonds are indicated by the dashed line.

and Asp/Glu V:-1 has a χ^1 angle of $-60°$ or $180°$ in complexes with cyclic peptides or complexes with other opiates, respectively. Furthermore, Tyr[312] (VII:3) in the κ opioid receptor has a χ^1 angle of $-60°$ for peptide and nonpeptide ligands, except for norbinaltorphimine (norBNI), which requires $\chi^1 \approx 180°$ to provide additional space for this bulky ligand.

The structures of the binding pockets were tested for complementarity to 16 rigid or conformationally constrained opioid ligands with very different chemical structures and sizes (Fig. 2). Peptides from the DPDPE and JOM-13 series were chosen because they have small rigid cycles and have been extensively studied by x-ray crystallography (Flippen-Andersen et al., 1994; Lomize et al.,

1994; Deschamps et al., 1996), NMR spectroscopy (Mosberg et al., 1990; Mosberg and Sobczyk-Kojiro, 1991; Collins et al., 1996), and theoretical methods (Froimowitz, 1990; Wilkes and Schiller, 1991). Larger linear and cyclic opioid peptides are too flexible to be useful for verification of receptor models. It was found that crystal structures of all ligands examined, except DPDPE, fit the pockets, with only a few flexible torsion angles, in some cases, needing to be adjusted (Tables 2 and 3). The largest ligands (such as DPDPE or norBNI) fill almost all of the available space within the binding cavities and interact with residues from both "conserved" and "variable " regions. Smaller alkaloids (such as morphine and naloxone), on the other hand, interact predominantly with "conserved" residues in the bottom of

FIGURE 7   Comparison of the δ-opioid receptor model transmembrane α-bundle (*blue*) and the EM-based model of Baldwin et al. (Baldwin, 1997) (*red*) (stereo view).
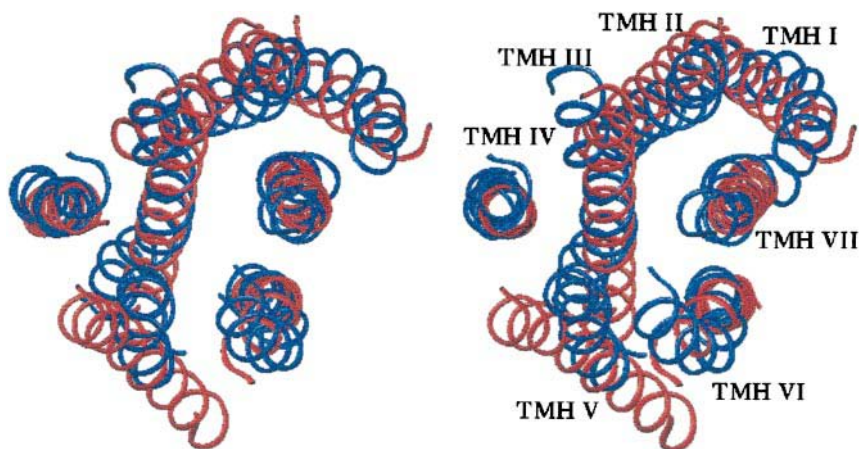
the binding cavity, leaving some free space around the ligand. The results of extensive structure-activity studies of JOM-13 and DPDPE analogs (Heyl and Mosberg, 1992a,b; Mosberg et al., 1994a,b; Haaseth et al., 1994) and mutagenesis data (Befort et al., 1996a,b; Hjorth et al., 1995; Meng et al., 1996; Pepin et al., 1997; Surratt et al., 1994; Valiquette et al., 1996) were used to verify the ligand docking.

The complementarity of rigid opiates and their binding pockets in the receptor models is evident from two different criteria. First there is a good geometrical fit; the ligands can be inserted in the bottom of the binding pocket without significant hindrances or holes in the area of contact. Second, and even more important, there is a spatial complementarity of groups with similar polarities, such that nearly all polar groups of the ligands form H-bonds with corresponding polar side chains within the binding pocket, whereas all ligand nonpolar (aliphatic and aromatic) groups form stabilizing hydrophobic contacts with nonpolar side chains of the receptors.

Cyclic peptides

The cyclic pentapeptide DPDPE (Tyr-c[D-Pen-Gly-Phe-D-Pen]OH) is a standard δ-selective ligand that is widely used in studies of opioid receptors (Mosberg et al., 1983). Its more constrained [D-Cys^2, *des*-Gly^3] (JOM-13) and [L-Ala^3] analogs have high δ affinities and selectivities, whereas [D-Ala^3]DPDPE is much less potent (Haaseth et al., 1994). JH-42 is a modified version of JOM-13 with Δ^EPhe^3 and an amidated C-terminus, modifications that result in a shift in binding selectivity from δ to μ (Ho, 1997). X-ray crystallography shows that DPDPE and [L-Ala^3]-DPDPE have different, unique structures of their tetrapeptide cycles (Flippen-Anderson et al., 1994; Collins et al., 1996; Deschamps et al., 1996), whereas JOM-13 is present in the crystal in two forms (A and B) of its 11-membered ring, which are similar, except for the configuration of the disulfide bridge (S-S torsion angles of 89° and −99°, respectively) (Lomize et al., 1994). In all crystal structures of these peptides, the Phe$^{3(4)}$ side chains have *gauche*$^+$ ($\chi^1 \approx -60°$) rotamers, but Tyr^1 orientations are varied (Deschamps et al., 1996). The crystal structures of DPDPE and related peptides are consistent with NMR spectroscopy solution data, indicating conformational rigidity of the cycles (Mosberg et al., 1990; Mosberg and Sobczyk-Koiro, 1991; Collins et al., 1996; Lomize et al., 1996). However, theoretical conformational analyses indicate the possibility of several alternative low-energy structures of the disulfide-bridged cycle in DPDPE (Froimowitz, 1990; Wilkes and Schiller, 1991). All exocyclic elements of these peptides are very flexible in aqueous solution, i.e., they have undefined angles ψ and χ^1 of Tyr^1, φ of D-Cys/Pen^2, and χ^1 of Phe$^{3(4)}$ (Mosberg et al., 1990; Mosberg and Sobczyk-Koiro, 1991; Lomize et al., 1994; Collins et al., 1996).

JOM-13

The cyclic tetrapeptide JOM-13 was positioned in the δ receptor-binding pocket, using crystal structures A and B of its 11-membered cycle, but with adjusted torsion angles for the exocyclic Tyr^1 residue and χ^1 of Phe^3. First, Tyr^1 was positioned in the bottom of the pocket to simultaneously form H-bonds between its N$^+$ and OH groups with O$^{\delta 1}$ of Asp^{128} (III:7) and N$^{\epsilon 2}$ of His^{278} (VI:20), respectively (the corresponding N...O distances are 2.7 and 3.1 Å, respectively, in the final model of the receptor-ligand complex). This can be done only in the *trans* ($\chi^1 \approx 180°$) orientation of the Tyr^1 side chain. Next, the *gauche*$^+$ orientation of Phe^3 ($\chi^1 = -60°$) was chosen based on SAR for JOM-13 analogs (Mosberg et al., 1994b, 1996). Then the spatial position of the disulfide-bridged 11-membered ring relative to the fixed Tyr^1 was adjusted by rotating torsion angles ψ of Tyr^1 and φ of D-Cys^2. The ring position was adjusted simply to remove all significant hindrances between the ring and surrounding receptor residues. The δ receptor-bound conformation thus determined is very close to crystal structure B of JOM-13, except for the configuration of the disulfide bridge (S-S torsion angle ≈ −90°), which corresponds to crystal structure A (Table 3).

The bound conformation of JOM-13 geometrically fits the binding pocket of the δ receptor and forms a number of complex-stabilizing H-bonds and hydrophobic contacts with surrounding receptor residues (Fig. 8). The binding pocket can be arbitrary divided into subsites that are complementary to smaller structural elements of JOM-13, i.e., its Tyr^1 residue, D-Cys^2-D-Pen^4 disulfide bridge, Phe^3 side chain, and C-terminal COO$^-$ group. The positively charged nitrogen of Tyr^1 is located in a relatively polar binding subsite formed by several H-bonded residues from helices II, III, and VII (Gln^{105}(II:24), Asp^{128}(III:7), Tyr^{129}(III:8), and His^{301}(VII:4)). The aromatic ring of Tyr^1 occupies the bottom of the cavity between Tyr^{129}(III:8), Met^{132}(III:11), Ile^{215}(V:4), Trp^{274}(VI:16), His^{278}(VI:20), Val^{281}(VI:23), Leu^{300}(VII:3), Cys^{303}(VII:6), and Ile^{304}(VII:7). There are a few small empty spaces around Tyr^1 in the pocket, which
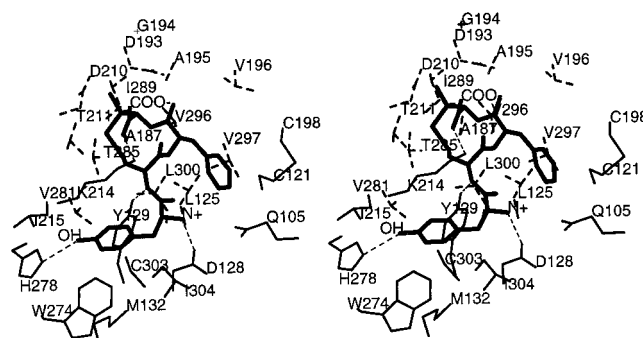

FIGURE 8　JOM-13 (*bold line*) inside the binding pocket of the δ-opioid receptor (stereo view). Conserved (*thin solid line*) and variable (*thin dashed line*) residues of the binding pocket (within 4.5 Å of the ligand) are also shown.

can accommodate methyl groups in the 2′ and 6′ positions of Tyr[1] and the extra ring of *trans*-Hpp[1] (*trans*-3-(4′-hydroxy)-phenylproline), consistent with the high affinities observed for the corresponding JOM-13 analogs (Mosberg et al., 1994a). On the other hand, the $C^{\alpha}H$-atom of Tyr[1] is in close contact with Tyr[129](III:8), and an additional C^{α}-methyl group incorporated here would experience steric hindrance with the aromatic ring of Tyr[129](III:8), consistent with the decreased affinities of αMeTyr[1], Hai[1] (6-hydroxy-2-aminoindan-2-carboxylic acid), and Hat[1] (6-hydroxy-2-aminotetralin-2-carboxylic acid) analogs of JOM-13 (Mosberg et al., 1994a). The Tyr[129](III:8) side chain also forms an $O^{\eta}\frac{1}{4}HN$ H-bond with the first peptide group of JOM-13, thus explaining the low affinity of [NMe-D-Cys[2]]JOM-13 (Heyl, 1991). Replacements of Tyr[1] by D-Tyr[1] and Tic[1] residues, which have entirely different orientations of the tyrosine ring within the pocket, produce numerous overlaps with surrounding receptor atoms, which correlates with the observed low binding affinities of D-Tyr[1] and Tic[1] analogs of JOM-13 (unpublished observations).

The disulfide bonded D-Cys[2]-D-Pen[4] pair of JOM-13 interacts primarily with the side chains of Thr[211](V:0), Thr[285](VI:27), Ile[289](VI:31), and Leu[300](VII:3). α-Methylation of Cys[2] is expected to decrease binding, because the αMe group would overlap with Leu[300](VII:3) in the model. This is in agreement with the reduced binding affinity found for [αMe-D-Cys[2]] JOM-13 (Heyl, 1991). The presence of empty spaces near the C^{β}-hydrogens of D-Cys[2] in the model is consistent with the comparable affinity observed upon replacement of D-Cys[2] by D-Pen[2] in analogs of JOM-13 (Mosberg et al., 1988).

The Phe[3] side chain of JOM-13 (conformer with $\chi^1 = -60°$) occupies the bottom of a rather large nonpolar cavity that is extended toward the extracellular side of the α-bundle and is covered by a β-hairpin formed by EL-2 (the aromatic ring of Phe[3] is located below the conserved Cys[121](III:0)-Cys[198](EL-2) disulfide bond and interacts with Gln[105](II:24), Leu[125](III:4), Val[297](VII:1), and His[301](VII:4); see Fig. 11). The presence of significant empty space in this cavity might allow a reorientation of the Phe[3] side chain from $\chi^1 = -60°$ to $\chi^1 = 180°$. In this case, the aromatic ring of Phe[3] would occupy an alternate position, above the disulfide bond, and would interact primarily with residues from EL-2 (Val[197], Cys[198]) and the extracellular terminus of TMH III (Glu[118](III:-3), Cys[121](III:0), Lys[122](III:1), Leu[125](III:4)). However, in the model, this would require a shift of the tripeptide ring system of JOM-13, which creates steric hindrances between Tyr[1] of the peptide and Tyr[129](III:8) of the receptor. Therefore, the preferred orientation of Phe in the δ receptor is *gauche* ($\chi^1 = -60°$), in agreement with the high affinities of [Δ^ZPhe[3]] and [(2R, 3S)MePhe[3]] analogs of JOM-13 (Mosberg et al., 1994b, 1996), in which the χ^1 angles of residue 3 are fixed in this orientation. The reduced δ binding affinity observed for [Δ^EPhe[3]]JOM-13, in which χ^1 of Phe[3] is fixed at 180° (Mosberg et al., 1996), is also consistent with the model. The size of the cavity in which the Phe[3] side chain

is situated can be increased even further if the Leu[125] (III:4) side chain assumes an alternative orientation, with a different χ^1 angle. In this case, the cavity can accommodate even larger side chains, such as those of Nal[3] (naphthylalanine) or Trp[3] in the same $\chi^1 = -60°$ orientation, consistent with the high affinity of the corresponding analogs of JOM-13 (Heyl and Mosberg, 1992a).

The C-terminal COO^- group of JOM-13 forms a H-bond with the ϵ amine of Lys[214](V:3) ($\chi^1 = -60°$, $\chi^2 = 180°$, $\chi^1 = 180°$, $\chi^1 = 180°$), buried inside the α-bundle. The ionic interaction between these oppositely charged groups is lacking for carboxamide terminal peptide ligands, such as the carboxamide analog of JOM-13, which displays a 10-fold reduction in δ binding affinity (Mosberg et al., 1988).

The δ bound conformation of JOM-13 determined here is in agreement with SAR studies of JOM-13 analogs with modified first and third residues (Mosberg et al., 1994a,b). These studies indicate that the Tyr[1] and Phe[3] side chains have *trans* and *gauche*[+] orientations, respectively; however, the conformation of the peptide group between Tyr[1] and D-Cys[2] is less defined. Two alternative conformers of JOM-13, with a φ angle of D-Cys[2] ~160° or ~70° were found to be energetically plausible and consistent with SAR data. Of these, the $\phi \approx 160°$ conformer was proposed to be the binding conformation, because it provided a better superposition of all pharmacophoric elements (Tyr[1] residue and Phe[3] side chain) in different analogs of JOM-13 (Mosberg et al., 1994a,b). However, it is clear from the ligand-receptor docking examined here that only the alternate $\varphi \approx 70°$ conformer can fit the binding pocket. Indeed, the receptor models show that a precise superposition of all pharmacophoric elements is not required and that, even in similar cyclic peptides, the functionally important phenylalanine aromatic ring may change orientation and location slightly, as further discussed below.

JH-42

Comparison of δ and μ receptor models explains some differences in δ versus μ selectivity among peptides from the JOM-13 series. For example, modification of the Phe[3] residue and amidation of the C-terminus of the δ-selective JOM-13 produces the μ-selective peptide JH-42 (Tyr-c[D-Cys-Δ^EPhe-D-Pen]NH$_2$). The parent peptide, JOM-13, fits the binding pocket of the δ receptor, interacting with Leu[300](VII:3). However, in the μ receptor model, the side chain of the Trp[318](VII:3) residue, which appears in place of Leu[300](VII:3) of the δ receptor, is partially overlapped with the tripeptide cycle of JOM-13 or its analog, JH-42. This causes a shift of the entire peptide within the binding pocket (Fig. 9), which, in turn, induces reorientation of the Phe[3] side chain from the *gauche*[+] to the *trans* χ^1 conformer to avoid steric overlap with Cys[140](III:0). As a result, the aromatic ring of Phe[3] is relocated in the μ receptor to the alternative spatial position above the conserved Cys[140](III:0)-Cys[217](EL-2) disulfide bond, between Thr[137](III:-3),

FIGURE 9 Superposition of δ and μ receptor models with inserted JOM-13 (*dark purple*) and JH-42 (*dark green*), respectively (stereo view). Receptor residues that are within 4.5 Å of the ligands and are different in δ and μ receptors are shown in light purple and light green, respectively. Lys²¹⁴⁽²³³⁾ is also shown, because it assumes different side-chain conformers in the δ and μ receptors. Numbering in the figure corresponds to the δ receptor.
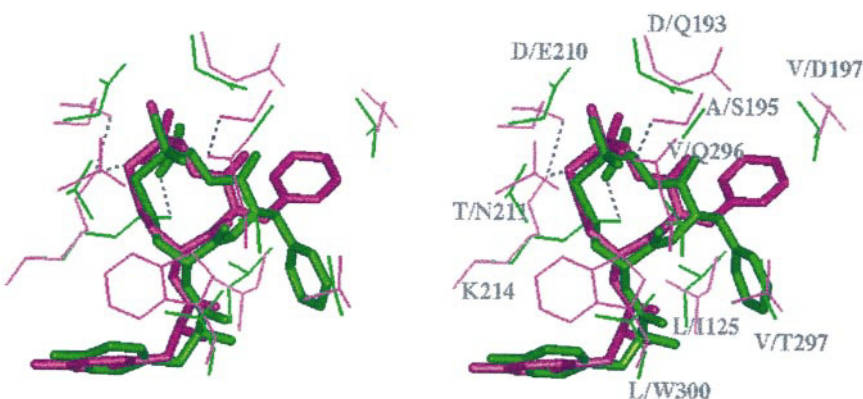
Cys¹⁴⁰(III:0), Lys¹⁴¹(III:1), Ile¹⁴⁴(III:4), Gln²¹²(EL-2), Asp²¹⁶(EL-2), and Cys²¹⁷(EL-2). Therefore, fixing the aromatic ring in this *trans* orientation via the Δ^{E}Phe³ modification in JH-42 improves affinity to the μ receptor.

The peptide C-terminus also interacts differently with δ and μ receptors. In the δ receptor model, the C-terminal COO⁻ group of JOM-13 forms an ion pair with the ε-amino group of Lys²¹⁴ (V:3), which is partially buried in the binding pocket. In the μ receptor model, the corresponding Lys²³³ (V:3) forms an ion pair with Glu²²⁹ (V:−1), which replaces the Asp found in the δ receptor. Because of the shifted position of the peptide ligand in the μ versus the δ receptor, noted above, the negatively charged peptide C-terminus makes contact with the COO⁻ group of Glu V:−1 in the μ receptor as well as with the ε-amino group of Lys V:3. Therefore, amidation of the C-terminus in JH-42, which removes the unfavorable electrostatic repulsion with the glutamic acid, improves μ binding, whereas incorporation of a negatively charged COO⁻ in JOM-13 improves δ binding.

[L-Ala³]DPDPE and DPDPE

X-ray crystallography studies (Deschamps et al., 1996) have led to the interesting observation that the crystal structures of two high-affinity analogs of DPDPE, the *des*-Gly³ analog, JOM-13, and [L-Ala³]DPDPE, are very similar to each other, but differ from the crystal structure of DPDPE itself (Lomize et al., 1996). Remarkably, all torsion angles of [L-Ala³]DPDPE, even including the flexible, exocyclic Tyr¹ residue and χ¹ of Phe, are close to those in crystal structure B of JOM-13, except for the angles of the disulfide bonds, which are nearly the same as in structure A of JOM-13 (Table 3). As a result, the crystal structure of [L-Ala³]DPDPE can be incorporated in the binding pocket of the δ opioid receptor exactly as is JOM-13, with almost identical positions of Tyr¹ residues, disulfide bonds, and C-terminal COO⁻ groups in both related peptides. Because of insertion of the Gly residue, the Phe⁴ aromatic ring in [L-Ala³]DPDPE is shifted by ∼3 Å (compared to that in JOM-13) toward the extracellular surface in the binding cavity.

In contrast to its [L-Ala³] analog, the crystal structure of DPDPE itself could not be incorporated in the receptor model, even with conformational adjustments of Tyr¹ and Phe³ residues. Incorporation of this crystal structure in the δ receptor model either breaks H-bonds of Tyr¹ with His²⁷⁸(VI:20), or produces strong steric hindrances between the 14-member ring of DPDPE and the receptor (this happens, in part, because the Tyr¹ and Phe⁴ side chains are too widely separated in the crystal structure of DPDPE). However, the alternative, "L-Ala³-like" conformer of DPDPE (Lomize et al., 1996) fits the binding pocket well. Thus the δ bound conformation of DPDPE is close to the crystal structures of its two high-affinity analogs, JOM-13 and [L-Ala³]DPDPE, which are more conformationally constrained than DPDPE itself.

Morphinans and benzomorphans

The positions of the largest rigid alkaloid ligands within the binding cavity are unequivocally defined by steric restrictions. For example, there is only one way in which the bulky bimorphinan norBNI (Portoghese et al., 1987) can be placed in the cavity of the κ receptor without the appearance of significant hindrances with surrounding receptor atoms. This docking mode simultaneously provides ionic interactions between the positively charged 17-N atom of norBNI and the COO⁻ group of Asp¹³⁸(III:7) (N. . . O$^{\delta d1}$ distance of 5.8 Å) and between the symmetrical 17′-N of norBNI and Glu²⁹⁷ (VI:26) of the κ receptor (N. . . O$^{\epsilon e1}$ distance of 3.1 Å), consistent with SAR studies of norBNI analogs (Portoghese et al., 1994) and mutagenesis experiments (Hjorth et al., 1995). At the same time, 17-N can form a H-bond with Tyr¹³⁸(III:8) or Tyr³¹²(VII:3), the 14-OH group of norBNI forms a H-bond with Tyr¹³⁹ (III:8), and the ligand's 14′-OH group H-bonds with Glu²⁹⁷ (VI:26) of the κ receptor.

In contrast, some small alkaloid ligands, such as morphine, can be arranged in several sterically allowed alternate positions in the pocket, all of which provide contact between the ligand N⁺ and AspIII:7 and which permit the formation of H-bonds between ligand and receptor polar groups. To satisfy SAR data, which suggest a similar functional importance and environment of specific ligand groups

common to a structural class, the general position of both small and large ligands of the same structural type (such as norBNI and morphine) were assumed to be similar, with only a small (<2 Å) vertical adjustment within the cavity allowed. Two slightly different positions of morphine in the binding cavity are demonstrated in Fig. 10. The first, "upper" position of morphine is closer to the extracellular surface; the tyramine moiety of morphine is in a position similar to that of Tyr[1] of opioid peptides, except that the N^+ group of the tyramine is slightly farther from the side-chain carboxylate group of Asp^{147}(III:7) (the $N^+ \cdots O^{\delta1}$ distance for morphine is 4.0 Å, compared with 2.7 Å for JOM-13). The 3-OH group of the morphine tyramine moiety forms a H-bond with $N^{\delta1}$ of His^{297} (VI:20) of the μ receptor. In the second, alternate, "lower" position, N^+ of morphine is located ~1.5 Å deeper in the pocket, and the entire ligand molecule is shifted ~2 Å toward TMH V. In this position, the side chain of Asp^{147} (III:7) in the μ receptor can change orientation (χ^1 changes from $-60°$ to $180°$) and form a H-bond with the N^+ of morphine; the N^+H hydrogen in ring D is oriented axially and is directed toward $O^{\delta1}$ of the Asp^{147}(III:7) (distance of 3 Å). Ring A of morphine in both positions interacts with Ile^{234}(V:4), Trp^{293}(VI:16), Ile^{296}(VI:19), Val^{300}(VI:23), and Cys^{321}(VII:6) side chains, and the 3-OH group of ring A is at a distance of 3.5 Å from $N^{\delta1}$ of His^{297}(VI:20) (Fig. 8). Ring D interacts with the side chains of the conserved Tyr^{148}(III:8), Met^{151}(III:11), and Ile^{322} (VII:7) residues. Ring C contacts the side chains of the conserved Lys^{233} (V:3) ($\chi^1 = -60°$, $\chi^2 = 180°$, $\chi^3 = -60°$, $\chi^4 = 180°$) and Tyr^{148}(III:8), and with the μ subtype-specific Asn^{230}(V:0) and Trp^{318}(VII:3).

Bulky substituents of morphine derivatives usually impose additional steric constraints and substantially decrease the degrees of freedom of the ligand inside the cavity. For most alkaloid antagonists with N-allyl and N-cyclopropyl-methyl substituents (naloxone, naltrindole (NTI), norBNI, β-funaltrexamine (β-FNA)), the "lower" spatial position is probably preferred because the ligand N-substituents, in their energetically preferred equatorial positions, can be geometrically arranged, without steric hindrances, in a narrow hydrophobic "cleft" between the side chains of AspIII:7, MetIII:11, TrpVI:16, IleVII:7, GlyVII:10, and TyrVII:11, whereas the polar groups of the alkaloids form

several H-bonds with surrounding polar side chains, including N^+H (ligand)$\cdots$ COO^- AspIII:7 and 14-OH (ligand)$\cdots$ O^η TyrIII:8. Indeed, the importance of the TyrIII:8 side chain and hydroxyl group for interaction with 14-OH groups of naloxone and NTI has been demonstrated recently by mutagenesis (Befort et al., 1996b).

Some morphinans with bulky substituents, such as the 14-acetamido group of 14β-(bromoacetamido)morphine (BAM), the N-phenethyl group of phenethylmorphine, or the N-oxy-cyclopropylmethyl group of bremazocine, can be geometrically arranged only in the "upper" position, because any other locations produce steric overlaps of the substituents with receptor side chains in the binding cavity. Moreover, the OH group that is attached to the N-cyclopropylmethyl substituent in bremazocine further stabilizes the ligand in the "upper" position in all opioid receptors by forming H-bonds with Gln^{124}II:24 and AspIII:7 side chains. In these ligands, the C_9-N_{17}-C_{18}-C_{19} dihedral angle, which defines the spatial position of the N-substituents (Fig. 2), is changed from $\sim180°$ (as in naloxone, NTI, and norBNI in the "lower" position) to $\sim-60°$ to geometrically fit the binding pocket. This positions the N-substituents closer to the extracellular side between the Leu/MetII:21, GlnIII:24, Ile/LeuIII:4, AspIII:7, IleVII:7, and TyrVII:11 side chains.

It is possible that functional antagonism in morphinan alkaloids originates from a combination of features, such as the presence of specific N-substituents, the "lower" location of the ligand, and the rotation of the receptor AspIII:7 side chain. It is noteworthy that all related alkaloids situated in the "upper" position, such as bremazocine and phenethyl-morphine, are agonists (Römer et al., 1980; Casy and Parf-itt, 1986). Moreover, all agonists described below (BW373U86, aryacetamides, and fentanyl analogs) and the cyclic peptides discussed previously are situated in the "upper" position that is associated with the $\chi^1 = -60°$ conformer of AspIII:7. Some possible suggestions about the mechanism of opioid antagonism can be made by analogy with rhodopsin. Physicochemical studies of rhodopsin indicate that a rigid body movement of TMHs III and VI probably takes place during photoactivation (Farrens et al., 1996; Sheikh et al., 1996; Shieh et al., 1997). This movement may disrupt the ionic interaction between Glu^{113} (III:3) and Lys^{296} (VII:11), which is usually treated as the key event in the activation of rhodopsin (Fahmy et al., 1995), because replacement of Glu^{113} (III:3) or Lys^{296} (VII:11) produces constitutively active mutants (Robinson et al., 1992). In all opioid and cationic amine receptors, this Glu$\cdots$Lys pair is replaced by the conserved pair of Asp(III:7) and Tyr(VII:11), connected by a H-bond. Tyr^{308} (VII:11) in the δ opioid receptor corresponds to Lys^{296} (VII:11) of rhodopsin, whereas Asp^{128} (III:7) is situated in TMH III, one turn away from the position of Glu^{113} (III:3) in rhodopsin. It has been shown that Asp^{117}(III:7) can also serve as a counterion of the retinal protonated Schiff base in rhodopsin (Zhukovsky et al., 1992). It can be proposed that the ionic interaction of AspIII:7 with the protonated amine of opioid agonists can trigger the movement of TMH III and
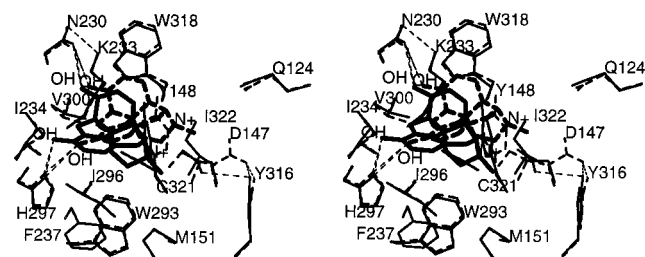

FIGURE 10   Two positions (*solid and dashed lines*) of ($-$)-morphine in the binding pocket of the μ-opioid receptor (stereo view). The ligand is denoted by the bold line, and receptor residues within 4.5 Å of the ligand by the thin line.

the rotation of the AspIII:7 side chain. *N*-Cyclopropyl-methyl and *N*-allyl substituents, characteristic of alkaloid opioid antagonists (Casy and Parfitt, 1986), are in close contact with TMH III in our models and may prevent its shift during activation, thus leading to functional antagonism. It is interesting to note that after superposition of opioid receptor and rhodopsin models, the *N*-cyclopropyl-methyl group of NTI and norBNI and the *N*-allyl group of naloxone spatially overlap with a fragment of the polyene chain (between the 9-methyl group and 11–12-*cis* double bond) of the natural "antagonist" of rhodopsin, 11-*cis*-retinal, which is more deeply embedded between the helices, than its "agonist" analog, the all-*trans* isomer of retinal (PDB files 1bok and 1 boj).

Comparison of the ligands docked in the models of the δ, μ, and κ opioid receptors also explains subtype selectivity for the morphinan alklaloids considered here. For example, the preferred binding of morphinans to the μ receptor can be explained by the presence of an additional H-bond between Asn[230](V:0) and the 6α-OH group of morphine (see Fig. 10) or the 6-keto group of naloxone (Asn[230] (V:0) is replaced by Thr and Leu in δ and κ receptors, respectively). The interaction of the Trp[318] (VII:3) ($\chi^1 = -60°$) aromatic ring with ring C can further contribute to the higher affinity of these ligands for the μ subtype (this Trp[318](VII:3) residue is replaced by Leu and Tyr in δ and κ receptors, respectively). On the other hand, the indole ring of the δ-selective antagonist NTI (Portoghese et al., 1987) (Fig. 2) interacts favorably with Thr[211] (V:0), Lys[214](V:3), Ile[289](VI:31), Val[296](VII:−1), Val[297](VII:0), and Leu[300] (VII:3) in the δ receptor model, but has substantial steric hindrances with the corresponding, more bulky Asn[230](V:0), Gln[314](VII: −1), and Trp[318](VII:3) in the μ receptor model, or Leu[224](V:0), Leu[309](VII:0), and Tyr[312] (VII:3) in the κ receptor model. This agrees with the observation that mutations of Val[297](VII:0) and Leu[300] (VII:3) decrease binding of NTI to δ receptor (Valiquette et al., 1996; Meng et al., 1996).

Piperazine derivatives (BW 373U86)

The recently discovered δ-selective agonist BW373U86 (Fig. 2), in the conformation corresponding to the crystal structure of its 3-F analog (Calderon et al., 1997; Table 2), properly fits the binding pocket of the δ opioid receptor (Fig. 11). The 3-hydroxybenzyl moiety of BW373U86 spatially corresponds to the A ring of morphine, but has a different orientation of its phenyl ring. The 3-hydroxy group of BW373U86 is pointed toward His[278] (VI:20) (O. . . N^{ε2} distance is 2.6 Å), one nitrogen of the piperazine moiety is close to the Tyr[129] (III:8) O^{η}H group (N. . . O distance is 3.3 Å), and the other, positively charged nitrogen interacts electrostatically with Asp[128] (III:7) ($\chi^1 = -60°$) (N. . . O^{δ1} distance is 4.0 Å). Like the *N*-allyl substituent of naloxone, the *N*-allyl group of BW373U86 forms favorable hydrophobic contacts with Asp[128] (III:7), Met[132](III:11), Ile[304](VII:
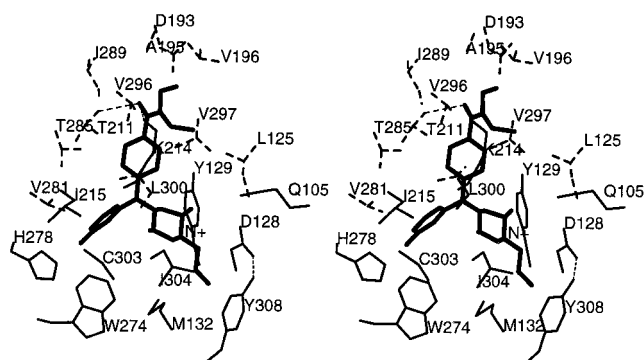

FIGURE 11   The δ-selective agonist BW373U86 (*bold line*) inside the binding pocket of the δ-opioid receptor (stereo view). Conserved (*thin solid line*) and variable (*thin dashed line*) residues of the binding pocket (within 4.5 Å of the ligand) are also shown.

7), and Tyr[308](VII:11). However, in BW373U86 the *N*-allyl group is shifted toward TMH II by ~1.5 Å compared with its position in morphinan antagonists. As a result, this group is situated between TMH III and VII, rather than between TMH III and VI as in antagonist naloxone, and does not interact with Trp[274](VI:16), which accounts for the agonist activity of BW373U86. The Asp[128] (III:7) side chain has the same orientation as in peptides. The diethylbenzamide fragment of BW373U86 interacts with residues at the extracellular ends of helices III, V, VI, and VII (Leu[125](III:4), Thr[211](V:0), Lys[214](V:3), Thr[285](VI:27), Ile[289](VI:31), Val[296](VII:−1), Val[297](VII:0), and Leu[300](VII:3)) and with Ala[195] from EL-2 of the δ receptor. This could explain the decreased affinity of BW373U86 analogs for δ receptor mutants with replacements for residues Ile[289](VI:31), Val[296](VII:−1), Val[297](VII:0), and Leu[300] (VII:3) (Valiquette et al., 1996; Pepin et al., 1997; Meng et al., 1996).

Fentanyl analogs

The μ-selective agonists *cis*-(+)-3-methylfentanyl and lofentanil (Fig. 2) were inserted into the binding pocket of the μ receptor model using, primarily, the crystal structure of *cis* (+)-3-methylfentanyl (Flippen-Anderson and George, 1994). In the crystal structure, the piperidine ring of fentanyl is in a chair conformation, the 4-phenylpropanamide substituents are in equatorial positions, and the *N*-phenethyl moiety is in an extended conformation (see Table 2 for dihedral angles). The docking of three different orientations of the *N*-phenethyl fragment, one extended (A) and two bent (B and C) (Table 2), was examined. The accommodation of structure A in the μ receptor model (Fig. 12) requires the rotation of the Gln[124](II:24) side chain, which exposes its amide bond to the lipid phase. This energetically unfavorable polarity mismatch seems unlikely. In conformation B the phenyl ring of the phenethyl fragment is closely packed between TMH II, III, and VII. In this orientation substituents on the phenyl ring cannot be accommodated, because of a lack of space between residues
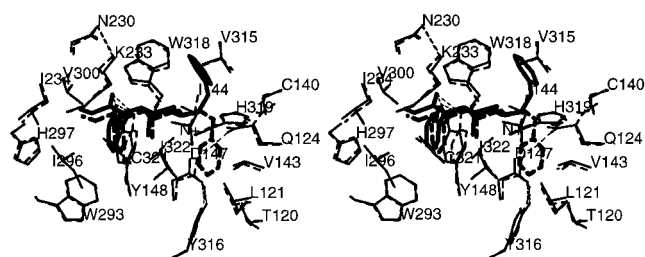
FIGURE 12   Two conformations of *cis*-(+)-3-methylfentanyl (B, dashed line; C, solid line) in the μ-opioid receptor (stereo view). The ligand is denoted by the bold line, and receptor residues within 4.5 Å of the ligand by the thin line.

FIGURE 13   The κ-selective alkaloid agonist U69,593 (*bold*) in the binding pocket of the κ-opioid receptor (stereo view). Conserved (*thin solid line*) and variable (*thin dashed line*) residues of the binding pocket within 4.5 Å of the ligand are also shown.

Asp[147] (III:7), Ile[322] (VII:7), and Tyr[316] (VII:11). Because such phenyl ring-substituted fentanyl analogs do indeed bind with high affinity (Casy and Parfitt, 1986; Zhu et al., 1996a), this orientation of the ligand is also unlikely. Thus conformation C, with the phenyl ring oriented toward the extracellular surface, is the most reasonable choice for the binding conformation of fentanyl analogs. In the C conformer, the phenyl ring of 3-methylfentanyl occupies the same spatial position as Phe[3] in the cyclic peptide JOM-13. In this conformation the 3-methylfentanyl is placed in the bottom of the binding cavity, and the positively charged piperidine nitrogen is close to $O^{\delta 1}$ of Asp[147](III:7) (N. . . $O^{\delta 1}$ distance is 3.7 Å; Fig. 8). The piperidine ring contacts Asp[147](III:7), Tyr[148](III:8), Trp[318](VII:3), and Ile[322](VII:7), and the carbonyl oxygen of the 3-methylfentanyl amide forms a H-bond with Lys[233] (V:3) and Tyr[148](III:8). The aromatic ring of the 4-phenylpropanamide moiety interacts with Ile[234](V:4), Trp[283](VI:16), Ile[296](VI:19), His[297](VI: 20), Val[300](VI:23), Cys[321](VII:6), and Ile[322](VII:7). The 3-methyl group of fentanyl analogs forms additional hydrophobic contact with Tyr[148](III:8) and Ile[322](VII:7) from helix VII, and the COOCH$_3$ group in position 4 of the piperidine ring of lofentanil forms a H-bond with Lys[233] (V:3) and Asn[230] (V:0), present only in the μ receptor. Fentanyl and its analogs can be readily positioned in the binding pocket of the δ receptor, but the lost favorable interaction with Trp[318] (VII:3) (replaced in the δ receptor by Leu[300](VII:3)) decreases the binding affinity. In the κ receptor, Tyr[313](VII:4) replaces His(VII:4) of δ and μ receptors, and has steric hindrances with fentanyl derivatives, consistent with the reduced binding affinity for this receptor subtype.

Arylacetamides

The majority of highly κ-selective agonists are derived from the prototype U50,488 (Szmuszkovicz and Von Voightlander, 1982), which is structurally unrelated to morphine congeners. As an example of this arylacetamide series, the second-generation analog U69,593 (Lahti et al., 1985) (Fig. 2) was inserted in the κ receptor model (Fig. 13). The crystal structure of the ligand (Doi et al., 1990) provides a good fit to the model. The pyrrolidine ring of U69,593 is
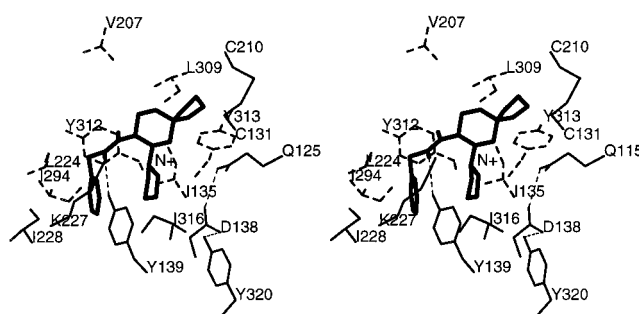
located between Asp[138](III:7), Tyr[139](III:8), and Ile[316](VII: 7), and the central ring system is oriented toward the extracellular side, interacting with residues from helices II, III, and VII (Glu[115](II:24), Ile[135](III:4), Leu[309](VII:0), and Tyr[313](VII:4)) and with the conserved Cys[131](III:0)-Cys[210](EL-2) disulfide. The benzacetamide group occupies the same region of space as the tyramine moiety of alkaloids, but oriented in a perpendicular direction. It forms contacts with residues Tyr[139](III:8), Leu[224](V:0), Ile[228](V: 4), Ile[294](VI:23), Tyr[312](VII:3), and Ile[316](VII:7). The carbonyl forms a H-bond with Tyr[139] (III:8) and is close to Lys[227] (V:3) (N. . . O distance = 3.7 Å). The interactions of this ligand with residues from many helices is consistent with mutagenesis data that reveal the importance of all helices for the binding of U69,593 to the κ receptor (Metzger and Ferguson, 1995). The selectivity of U69,593 for the κ receptor subtype appears to result from the presence of the κ receptor-specific residues in helices V–VII (Leu[224](V:0), Ile[294](VI:23), Leu[309](VII:0), Tyr[312](VII:3), and Tyr[313](VII:4)), which modify the shape of the binding pocket.

Affinity labels

The δ, μ, and κ receptor models were tested further by examining irreversible ligands that covalently attach to specific residues in the binding pockets. The μ-affinity label β-FNA (Fig. 2) was positioned in the μ receptor model, like to the parent morphine in the "lower" position (Fig. 10), with the fumarate double bond within 3.0 Å of the ε-amine of Lys[233] (V:3), allowing covalent attachment. Recently, chimera studies and site-directed mutagenesis have demonstrated that Lys[233] (V:3) is indeed the site of μ-specific irreversible binding of β-FNA (Chen et al., 1996). β-FNA irreversibly modifies μ receptors but binds reversibly to κ and, with lower affinity, to δ receptors (Takemori and Portoghese, 1985). This results from the existence of different conformers of the LysV:3 side chain in μ, δ, and κ receptors. In μ receptors Lys[233] (V:3) forms a H-bond with Glu[229] (V:−1) and adopts a conformer ($\chi^1 = -60°$, $\chi^2 = 180°$, $\chi^3 = -60°$, $\chi^4 = 180°$) that positions the ε-amine

group of the lysine near the fumarate double bond of the affinity label. However, the Glu V:−1 residue is replaced by Asp in δ and κ receptors. In the models of receptor–β-FNA complexes, Lys V:3 can still form a H-bond with the shorter side chain of the corresponding Asp V:−1, but this requires a different conformer of the side chain: χ^3 of Lys V:3 must be changed from −60° to 180°. In this conformer, the distance between the ϵ-amine of LysV:3 and the fumarate double bond of the ligand is increased (>5.0 Å) such that covalent attachment does not occur. In addition, the β-branched Thr^{211}(V:0) in the δ receptor sterically interferes with β-FNA, substantially decreasing the ligand affinity.

The δ-selective ligand SUPERFIT (*cis*-(+)-3-methylfentanyl isothiocyanate) (Fig. 2) was positioned in the δ model as in the parent fentanyl in conformation C (Fig. 12). In this arrangement, the *p*-isothiocyanate of SUPERFIT can form a covalent bond with the ϵ-amino group of Lys^{122} (III:1) ($\chi^1 = -60°$, $\chi^2 = -60°$, $\chi^3 = -60°$), which is located near by (distance between N$^\epsilon$ of Lys^{122}(III:1) and S of the ligand is 2.7 or 4.7 Å for χ^4 of Lys^{122}(III:1) = 180° or $\chi^4 = 60°$, respectively). This is in agreement with receptor chimera studies which indicate that SUPERFIT is covalently attached to a residue in the region 76–134 of the δ receptor (Zhu et al., 1996a). Although LysIII:1 is a common residue for δ, μ, and κ receptor subtypes, SUPERFIT selectively modifies δ receptors. As in the case of selective labeling of μ receptors by β-FNA discussed above, the δ selectivity of SUPERFIT results from different environments and different rotamers of LysIII:1 in different receptor subtypes (see H-bonds with LysIII:1 in different receptors, shown in Table 1).

BAM (Fig. 2) is a sulfhydryl alkylating reagent that specifically labels μ-opioid receptors after reduction of an unidentified disulfide bond close to the binding site (Bidlack et al., 1989). To avoid steric hindrances between the acetamido group of BAM and the Tyr^{148}(III:8) side, the ligand was positioned in the μ receptor model in the same fashion as its congener phenethylmorphine (see the "upper" position of morphine, represented by the *dashed line* in Fig. 10). In the receptor bound complex, the 14β-bromoacetamido group of BAM is close to Cys^{140}(III:0) (distance between Br and C$^\beta$ of Cys^{140}(III:0) is 6.1 Å). Our model thus predicts that it is the SH group of Cys^{140} (III:0) that becomes available for modification by BAM after reduction of the Cys^{140}(III:0)-Cys^{217}(EL-2) disulfide bond by dithiothreitol.

The κ-selective labeling reagent 2-(3,4-dichlorophenyl)-N-methyl-N-[1-(3-isothiocyanatophenyl)-2-(1-pyrrolidinyl) ethyl] acetamide (DIPPA) (Fig. 2) was inserted into the binding pocket of the κ receptor model in a conformation similar to its x-ray structure (Chang et al., 1994) and similar to the binding mode of U69,593. The 3-isothiocyanate group of DIPPA is near Lys^{132} (III:1) (distance between N$^\epsilon$ of Lys^{132} (III:1) and S of DIPPA is 2.8 Å), and is likely to modify its ϵ-amino group.

Mutagenesis data

The opioid receptor models are generally consistent with published SAR data for their ligands, covalent labeling, and mutagenesis data. The site-directed mutagenesis data can be divided into two groups. The first group includes mutagenesis of residues that are near the binding pocket of the calculated models. Replacement of many residues in the "conserved" region of the binding pocket, which are involved in the models in the formation of H-bonds with polar groups of the ligands, affects the binding of numerous ligands from different structural classes (Befort et al., 1996a,b; Chakrabarti et al., 1997; Surratt et al., 1994; Mansour et al., 1997). In particular, in all opioid receptor models, AspIII:7 forms the ionic pair or hydrogen bond with N$^+$ of all opioid ligands. This correlates with the deleterious effect of the AspIII:7→Asn substitution on receptor activation and the binding of ligands, especially agonists (morphine, bremazocine, and peptides), to μ and δ receptors (Surratt et al., 1994; Befort et al., 1996a). Furthermore, TyrIII:8, TrpVI:16, and HisVI:20, whose mutations have been demonstrated to affect ligand binding (Befort et al., 1996b; Surratt et al., 1994; Mansour et al., 1997), interact directly with different ligands in the models: TyrIII:8 forms a H-bond with the first peptide group of JOM-13 and other cyclic peptides and with the 14-OH group of morphinans; HisVI:20 forms a H-bond with the hydroxyl group of Tyr^1 of peptides and the tyramine moiety of alkaloids; TrpVI:16 interacts with the aromatic ring of Tyr^1 or ring A of alkaloids. The effect of Tyr(VII:11) substitution on ligand binding (Mansour et al., 1997) can be explained by its participation in the H-bond network with Asp(III:7), the key residue for electrostatic interaction with N$^+$ of all opioid ligands. Mutations in the "variable" region of the pocket, especially of residues from the extracellular ends of helices VI and VII in δ receptors (Val^{281}(VI:23), Trp^{284}(VI:26), Ile^{289}(VI:31), Arg^{291}(EL-3), Arg^{292}(EL-3), Val^{296}(VII:-1), Val^{297}(VII:0), and Leu^{300} (VII:3)), which contact the disulfide ring of δ-selective cyclic peptides, the diethylbenzamide fragment of BW373U86, and the indole ring of naltrindole, corroborate the importance of this region for selective binding of δ-ligands (Valiquette et al, 1996; Pepin et al., 1997; Meng et al., 1996). The formation of H-bonds between 14′-N$^+$ and 3′-OH of norBNI and Glu^{297} (VI:26) in the κ receptor model correlate with the important role of Glu^{297} (VI:26) for selective binding of norBNI to the κ receptor, suggested from mutagenesis results (Hjorth et al., 1995). Certainly the effect of the same replacement on binding of different ligands may vary significantly, because the energy of the receptor-ligand interaction depends on the structure of the ligand and on its precise position relative to the mutated residue. As described above, ligands of different structure and size interact with different sets of residues and have slightly different positions in the binding pocket, although they occupy the same cavity between TMHs III, IV, V, V, and VII.

The second set of data includes mutagenesis of residues that are remote from the binding pocket in our models. Replacements of many residues, located between helices II and III and between helices VI and VII in this set, have negligible effects (Fukuda et al., 1995; Minami et al., 1996; Valiquette et al., 1996), but others (AspII:14, Lys/AsnII:27, TprIV:11, SerIV:15, PheV:11) can strongly affect the binding of opioid ligands (Surratt et al., 1994; Kong et al., 1994; Chakrabarti et al., 1997; Claude et al., 1996; Befort et al., 1996b; Fukuda et al., 1995; Minami et al., 1996). In our model, all residues indirectly affecting ligand binding are tightly packed at the helix-helix interfaces, and most of them (AspII:14, Lys/AsnII:27, TrpIV:11, SerIV:15) also form interhelical H-bonds (see Table 1). The replacement of such tightly packed residues by residues of different volume and/or H-bonding capability is expected to produce shifts of entire helices, as is always observed in similar mutagenesis studies of buried, core residues in α-helical proteins (Daopin et al., 1991; Eriksson et al., 1992; Baldwin et al., 1993, 1996), or during the natural evolution of α-helical proteins (Lesk and Chothia, 1980; Chothia and Lesk, 1985a,b). The shifts of the α-helices can, in turn, affect ligand binding. Thus, for example, the deleterious effect on binding observed when the bulky Phe[222] (V:11) and Trp[173] (IV:11) residues are replaced by Ala in the δ receptor (Befort et al., 1996b) can be expected. Similarly, replacement of Lys[108] (II:27) (Fukuda et al., 1995; Minami et al., 1996), which forms H-bonds between its ϵ-NH$_3^+$ group and two main-chain C=O groups from EL-1 and EL-2, can induce conformational changes in the loops, indirectly affecting binding of ligands, especially large ones, such as DPDPE and other peptide ligands, which strongly interact with EL-2 in the models.

Some of the remote mutations can be expected to affect the stabilities of the inactive and active receptor states differently, and therefore have different effects on the binding of agonists and antagonists. For example, replacement of Ser[177] (IV:15) in δ opioid receptor by Leu produces a mutant that can be activated by antagonists (Claude et al., 1996). In our model, this replacement is expected to shift TMH III relative to TMH IV, because there is no space between the H-bonded Thr[134] (III:13) and Ser[177] (IV:15) available for the more bulky Leu side chain. The shift of helix III has previously been suggested as an activation step, based on mutagenesis and physicochemical studies of rhodopsin (Sakmar and Fahmy, 1995; Shieh et al., 1997; Sheikh et al., 1996; Farrens et al., 1996); therefore the helix movement induced by Ser[177](IV:15)→Leu mutation may facilitate the activation process. Such a shift of the helices can be expected by analogy with all other α-helical proteins studied, where it has been shown that incorporation of a single, more bulky residue in the tightly packed protein core can never be relieved by rotating side chains or distorting rigid α-helix geometry, but requires helix movements (Daopin et al., 1991; Baldwin et al., 1993, 1996).

Another interesting example is the mutation of the conserved aspartate in helix II (AspII:14→Asn, Ala) in δ and μ receptors, which decreases binding of agonists but not antagonists and affects activation of G-proteins (Kong et al., 1993; Surrat et al., 1994; Chakrabarti et al., 1997). This Asp[95](II:14) residue has been implicated in the binding of Na$^+$ to the δ opioid receptors, because the presence of sodium ions affects agonist (but not antagonist) binding in the native but not in the D95N mutant receptor (Kong et al., 1993). In our δ opioid receptor model, Asp[95](II:14) participates in a H-bond network with the polar residues Asn[131](III:10), Ser[135](III:14), Ser[311](VII:14), and Asn[314] (VII:17) (Table 1), which, together with a water molecule, can coordinate the sodium ion (Lomize et al., 1998). The binding of Na$^+$ is expected to distort the H-bond network, as do the D95N, A mutations. The presence or absence of these H-bonds may be associated with the active and inactive states of the receptors, respectively, which would explain the lack of effect of the D95N mutation and Na$^+$ binding affect on antagonist binding.

From the above discussion it can be seen that all three opioid receptor models are in qualitative agreement with published mutagenesis data. A more detailed, quantitative comparison of the opioid receptor models with mutagenesis results is not feasible, because this requires the prediction of structural consequences of single-site mutations, which sometimes produce significant conformational changes in proteins (Louie and Brayer, 1989; Houset et al., 1991; Sauer et al., 1992), and the calculation of free energies of receptor-ligand interactions, which in itself is a very challenging problem (Kollman, 1993).

CONCLUSIONS

The δ, μ, and κ opioid receptor structures described here represent specific examples of our recently developed general model of the 7-α-helical transmembrane domain, calculated by iterative distance geometry refinement to provide saturation of "H-bonding potential" simultaneously in 410 different GPCRs. The structures of the extracellular loops proposed here are more tentative and require experimental verification; however, there are several arguments in support of the calculated models. First of all, the model is consistent with general principles of protein structure: it provides formation of a single continuous "minicore" of 43 evolutionarily conserved GPCR residues, merges side chains with similar polarities into clusters, and allows numerous correlated replacements of spatially close side chains, which is necessary to maintain close packing within the transmembrane domain (Lomize et al., 1998). The second indicator of the validity of the general model stems from the excellent agreement of the bovine rhodopsin model, which we have previously described, with a vast sample of physicochemical data available for this prototypical GPCR (Pogozheva et al., 1997). The third verification of the model, described in the present work, comes from ligand docking. The opioid receptor models were calculated here solely from H-bonding constraints, using no informa-

tion about their ligands. Nevertheless, the models have binding pockets that match crystal structures of different rigid opiates, including alkaloids, arylacetamides, pirerazine and piperidine analogs, and small cyclic peptides, as described in the "ligand binding" section above. Moreover, the calculated models are in agreement with affinity labeling studies of opioid receptors. In particular, the models demonstrate that, in the μ receptor model, β-FNA can modify Lys^{233} (V:3) and BAM can alkylate Cys^{140} (III:0) after reduction of the conserved S-S bond between Cys^{140} (III:0) and Cys^{217} (EL-2) by dithiothreitol, SUPERFIT can be attached to Lys^{122} (III:1) in the δ receptor model, and DIPPA can covalently modify Lys^{132} (III:1) in the κ receptor model.

Like rhodopsin, the structures of opioid receptors have only one binding cavity in which all agonists and antagonists can be arranged in a similar although not identical way. The common "message" (Portoghese et al., 1990) tyramine moiety of alkaloids, or Tyr^1 of cyclic peptides lies at the bottom of the binding cavity and interacts primarily with residues that are common to all opioid receptors. The N$^+$ and OH groups of the tyramine, or Tyr^1, form H-bonds with AspIII:7 and HisVI:20 receptor residues, respectively, even though the exact spatial positions of these ligand groups vary by 0.5–4.3 Å, depending on the ligand. The chemically different "address" fragments of the ligands (such as the indole group of NTI, or the oligopeptide cycle of DPDPE) are oriented perpendicular to the tyramine fragment, toward the extracellular surface of the transmembrane domain, and interact with many residues that differ among the δ, μ, and κ receptors and are situated along the "walls" of the binding cavity, or in the extracellular loops. Thus the spatial distribution of conserved and subtype-specific residues in the model match the "message" and "address" fragments of opiates.

There are several features that distinguish alkaloid agonists and antagonists: the antagonists are shifted slightly deeper in the binding pocket; they have an N-substituent of characteristic size inserted between TMH III and TMH VI; and antagonist binding probably requires rotation of the AspIII:7 side chain, which interacts with the N$^+$ group of both agonists and antagonists. The incorporation of a bulky N-terminal group between TMH III and TMH VI may sterically prevent the shift of these helices relative to each other during activation, thus leading to functional antagonism. The rigid body movement of TMHs III and VI during activation is suggested by recent physicochemical studies and by site-directed mutagenesis of bovine rhodopsin (Farrens et al., 1996; Sheikh et al., 1996; Shieh et al., 1997).

The structures of δ, μ, and κ receptors with JOM-13, ($-$)-morphine, and U69,593, respectively, have been deposited in the PDB database. Structures of other receptor-ligand complexes described here are available from the authors upon request.

REFERENCES

Alkorta, I., and G. Loew. 1996. A 3D model of the δ opioid receptor and ligand-receptor complexes. *Protein Eng.* 9:573–583.

Baldwin, E. P., O. Hajiseyedjavadi, W. A. Baase, and B. W. Matthews. 1993. The role of backbone flexibility in the accomodation of variants that repack the core of T4 lysozyme. *Science.* 262:1715–1718.

Baldwin, E., J. Xu, O. Hajiseyedjavadi, W. A. Baase, and B. W. Matthews. 1996. Thermodynamic and structural compensation in "size-switch" core repacking variants of bacteriophage T4 lysozyme. *J. Mol. Biol.* 121:542–559.

Baldwin, J. M. 1993. The probable arrangement of the helices in G protein-coupled receptors. *EMBO J.* 12:1693–1703.

Baldwin, J. M. 1997. An alpha-carbon template for the transmembrane helices in the rhodopsin family of G-protein-coupled receptos. *J. Mol. Biol.* 272:144–164.

Ballesteros, J. A., and H. Weinstein. 1995. Integrated methods for the construction of three dimensional models and computational probing of structure-function relations in G protein-coupled receptors. *Methods Neurosci.* 25:366–427.

Barlow, D. J., and J. M. Thornton. 1988. Helix geometry in proteins. *J. Mol. Biol.* 201:601–619.

Befort, K., L. P. Tabbara, S. Bausch, C. Chavkin, C. Evans, and B. L Kieffer. 1996a. The conserved aspartate residue in the third putative transmembrane domain of the δ-opioid receptor is not the anionic counterpart for cationic opiate binding but is a constituent of the receptor binding site. *Mol. Pharmacol.* 49:216–223.

Befort, K., L. P. Tabbara, D. Kling, B. Maigret, and B. L. Kieffer. 1996b. Role of aromatic transmembrane residues of the δ-opioid receptor in ligand recognition. *J. Biol. Chem.* 271:10161–10168.

Bernstein, F. C., T. F. Koetzle, G. J. Williams, E. E. Meyer, M. D. Brice, J. R. Rodgers, O. Kennard, T. Shimanouchi, and M. Tasumi. 1977. The Protein Data Bank: a computer-based archival file for macromolecular structures. *J. Mol. Biol.* 112:535–542.

Bidlack, J. M., D. K. Frey, A. Seyed-Mozaffari, and S. Archer. 1989. 14-β-(Bromoacetamido)morphine irreversible labels μ-opioid receptor in rat brain membranes. *Biochemistry.* 28:4333–4339.

Brooks, B. R., E. R. Bruccoleri, E. R. Olafson, D. J. States, S. Swaminathan, and M. Karplus. 1983. CHARMM: a program for macromolecular energy, minimization and dynamics calculations. *J. Comput. Chem.* 4:187–217.

Bye, E. 1976. The crystal structure of morphine hydrate. *Acta Chem. Scand.* B30:549–554.

Calderon, S. N., K. C. Rice, R. B. Rothman, F. Porreca, J. L. Flippen-Anderson, H. Kayakiri, H. Xu, K. Beckets, L. E. Smith, E. J. Bilsky, P. Davis, and R. Horvath. 1997. Probes for narcotic receptor mediated phenomena. 23. Synthesis, opioid receptor binding, and bioassay of the highly selective δ agonist ($+$)-4-[(αR)-α-((2S,5R)-4-allyl-2,5-dimethyl-1-piperazinyl)-3-methoxybenzyl]-*N,N*-diethylbenzamide (SNC 80) and related novel nonpeptide δ opioid receptor ligands. *J. Med. Chem.* 40:695–704.

Cappelli, A., M. Anzini, S. Vomero, C. M. Menziani, P. G. De-Benedetti, M. Sbacchi, G. D. Clarke, and L. Mennuni. 1996. Synthesis, biological evaluation, and quantitive receptor docking simulation of 2-[(acylamino)ethyl]-1,4-benzodiazepines as novel tifluadom-like ligands with high affinity and selectivity for κ-opioid receptors. *J. Med. Chem.* 39:860–872.

Casy, A. F., and R. T. Parfitt. 1986. Opioid Analgesics: Chemistry and Receptors. Plenum Press, New York.

Chakrabarti, S., W. Yang, P. Y. Law, and H. H. Loh. 1997. The mu-opioid receptor down-regulates differently from the delta-opioid receptor: requirement of a high affinity receptor/G protein complex formation. *Mol. Pharmacol.* 52:105–113.

Chang, A.-C., A. E. Takemori, W. H. Ojala, W. B. Gleanson, and P. S. Portoghese. 1994. κ-Opioid receptor selective affinity labels, electro-

philic benzeneacetamides as κ-selective opioid antagonists. *J. Med. Chem.* 3:4490–4498.

Chen, C., J.-C. Xue, J. Zhu, Y.-W. Chen S, P. Kunapuli, J. K. de Riel, L. Yu, and L.-Y. Liu-Chen. 1995. Characterization of irreversible binding of β-funaltrexamine to the cloned rat μ-opioid receptor. *J. Biol. Chem.* 270:17866–17870.

Chen, C., J. Y. Yin, J. K. de Riel, R. L. DesJarlais, L. F. Raveglia, J. Zhu, and L-Y. Lui-Chen. 1996. Determination of the amino acid residues involved in [³H]β-funaltrexamine covalent binding in the cloned rat μ-opioid receptor. *J. Biol. Chem.* 271:21422–21429.

Chothia, C., and A. M. Lesk. 1985a. Helix movements and the reconstruction of the haem pocket during the evolution of the cytochrome *c* family. *J. Mol. Biol.* 182:151–158.

Chothia, C., and A. M. Lesk. 1985b. Helix movements in proteins. *Trends Biochem. Sci.* 10:116–119.

Claude, P. A., D. R. Wotta, X. H. Zhang, P. L. Prather, T. M. McGinn, L. J. Erickson, H. H. Lon, and P. Y. Law. 1996. Mutation of a conserved serine in TM4 of opioid receptors confers full agonistic properties to classical antagonists. *Proc. Natl. Acad. Sci. USA.* 93:5715–5719.

Collins, N., J. L. Flippen-Andersen, R. C. Haaseth, J. R. Deschamps, C. George, K. Kövér, and V. J. Hruby. 1996. Conformational determinants of agonist versus antagonist properties of [D-Pen², D-Pen⁵]enkephalin (DPDPE) analogs at opioid receptors. Comparison of X-ray crystallographic structure, solution ¹H NMR data, and molecular dynamic simulation of [L-Ala³]DPDPE and [D-Ala³]DPDPE. *J. Am. Chem. Soc.* 118:2143–2152.

Daopin, S., T. Alber, W. A. Baase, J. A. Wozniak, and B. W. Matthews. 1991. Structural and thermodynamic analysis of the packing of two α-helices in bacteriophage T4 lysozyme. *J. Mol. Biol.* 221:647–667.

Davies, A., G. F. X. Schertler, B. E. Gowen, and H. R. Saibil. 1996. Projection structure of an invertebrate rhodopsin. *J. Struct. Biol.* 117: 36–44.

deAlba, E., M. A. Jiménez, M. Rico, and J. Nieto. 1996. Conformational investigation of designed short linear peptides able to fold into β-hairpin structures in aqueous solution. *Folding Design.* 1:133–144.

Deisenhofer, J., and H. Michel. 1991. Structures of bacterial photosynthetic reaction centers. *Annu. Rev. Cell Biol.* 7:1–23.

Deschamps, J. R., C. George, and J. L. Flippen-Anderson. 1996. Structural studies of opioid peptides: a review of recent progress in x-ray diffraction studies. *Biopolymers.* 40:121–139.

Dhawan, B. N., F. Cesselin, R. Raghubir, T. Reisine, P. B. Bradley, P. S. Portoghese, and M. Hamon. 1996. International Union of Pharmacology. XII. Classification of opioid receptors. *Pharmacol. Rev.* 48:567–592.

Doi, M., T. Ishida, and M. Inoue. 1990. Conformational characteristics of opioid κ-receptor agonist: crystal structure of (5S,7S,8S)-(−)-N-methyl-N-[7-(1-pyrrolidinyl)-1-oxaspiro[4.5]dec-8-yl]benzeneacetamide (U69, 593), and conformational comparison with some κ-agonists. *Chem. Pharm. Bull.* 38:1815–1818.

Donnelly, D., J. B. C. Findlay, and T. L. Blundell. 1994. The evolution and structure of aminergic G protein-coupled receptors. *Receptors Channels.* 2:61–78.

Elling, C. E., S. M. Nielsen, and T. W. Schwartz. 1995. Conversion of antagonist-binding site to metal-ion site in the tachikinin NK-1 receptor. *Nature.* 374:74–77.

Eriksson, A. E., W. A. Baase, X.-J. Zhang, D. W. Heinz, M. Blaber, E. P. Baldwin, and B. W. Matthews. 1992. Response of a protein structure to cavity-creating mutations and its relation to the hydrophobic effects. *Science.* 255:178–183.

Fahmy, K., F. Siebert, and T. P. Sakmar. 1995. Photoactivated state of rhodopsin and how it can form. *Biophys. Chem.* 56:171–181.

Farrens, D. L., C. Altenbach, K. Yang, W. L. Hubbell, and H. G. Khorana. 1996. Requirement of rigid-body motion of transmembrane helices for light activation of rhodopsin. *Science.* 274:768–770.

Fernandez, L. M., and D. Puett. 1996. Lys⁵⁸³ in the third extracellular loop of the lutropin/choriogonadotropin receptor is critical for signaling. *J. Biol. Chem.* 271:925–930.

Flippen-Anderson, J. L., and C. George. 1994. X-ray structure of potent opioid receptor ligands: etonitazene, *cis*-(+)-3-methylfentanyl, etorphine, diprenorphine, and buprenorphine. *Heterocycles.* 39:751–766.

Flippen-Anderson, J. L., V. J. Hruby, N. Collins, C. George, and B. Cudney. 1994. X-ray structure of [D-Pen², D-Pen⁵]enkephalin, a highly potent, δ opioid receptor-selective compound: comparisons with proposed solution conformations. *J. Am. Chem. Soc.* 116:7523–7531.

Fraser, C. M., C.-D. Wang, D. A. Robinson, J. D. Gocayne, and J. C. Venter. 1989. Site-directed mutagenesis of m1 muscarinic acetylcholine receptors: conserved aspartic acids play important roles in receptor function. *Mol. Pharmacol.* 36:840–847.

Froimowitz, M. 1990. Conformational search in enkephalin analogues containing a disulfide bond. *Biopolymers.* 30:1011–1025.

Fu, D., J. A. Ballesteros, H. Weinstein, J. Chen, and J. A. Javitch. 1996. Residues I the seventh membrane-spanning segment of the dopamine D2 receptor accessible in the binding-site crevice. *Biochemistry.* 35: 11278–11285.

Fukuda, K., K. Terasako, S. Kato, and K. Mori. 1995. Identification of the amino acid residues involved in selective agonist binding in the first extracellular loop of the δ- and μ-opioid receptors. *FEBS Lett.* 373: 177–181.

Griffin, J. F., D. L. Larson, and P. S. Portoghese. 1986. Crystal structure of α- and β-funaltrexamine: conformational requirements of the fumaramate moiety in the irreversible blockage of μ opioid receptors. *J. Med. Chem.* 29:778–783.

Grigorieff, N., T. A. Ceska, K. H. Downing, J. M. Baldwin, and R. Henderson. 1996. Electron-crystallographic refinement of the structure of bacteriorhodopsin. *J. Mol. Biol.* 259:393–421.

Güntert, P., W. Brawn, and K. Wüthrich. 1991. Efficient computation of three-dimensional protein structure in solution from NMR data using the program DIANA and the supporting programs CALIBA, HABAS and GLOMSA. *J. Mol. Biol.* 217:517–530.

Güntert, P., and K. Wüthrich. 1991. Improved efficiency of protein structure calculations from NMR data using the program DIANA with redundant dihedral angle constraints. *J. Biomol. NMR.* 1:447–456.

Haaseth, R. C., P. J. Horan, E. J. Bilsky, P. Davis, T. Zalewska, J. Slaninova, H. I. Yamamura, S. J. Weber, T. P. Davis, F. Porreca, and V. J. Hruby. 1994. [L-Ala³]DPDPE: a new enkephalin analog with unique receptor activity profile. Further evidence of δ-opioid receptor multiplicity. *J. Med. Chem.* 37:1572–1577.

Habibi-Nezhad, B., M. Hanifian, and M. Mahmoudian. 1996. Computer-aided receptor modeling of human opioid receptors (mu, kappa and delta). *J. Mol. Model.* 2:362–369.

Han, M., S. W. Lin, M. Minkova, S. O. Smith, and T. P. Sakmar. 1996a. Functional interaction if transmembrane helices 3 and 6 in rhodopsin. Replacement of phenylalanine 261 by alanine causes reversion of phenotype of a glycine 121 replacement mutant. *J. Biol. Chem.* 271: 32337–32342.

Han, M., S. W. Lin, S. O. Smith, and T. P. Sakmar. 1996b. The effects of amino acid replacements of glycine 121 on transmembrane helix 3 of rhodopsin. *J. Biol. Chem.* 271:32330–32336.

Henderson, R., J. M. Baldwin, T. A. Ceska, F. Zemlin, E. Beckmann, and K. H. Downing. 1990. Model for the structure of bacteriorhodopsin based on high-resolution electron cryo-microscopy. *J. Mol. Biol.* 213:899–929.

Herzyk, P., and R. E. Hubbard. 1995. Automated method for modeling seven-helix transmembrane receptors from experimental data. *Biophys. J.* 69:2419–2442.

Heyl, D. L. 1991. Structural requirements for substitutions in delta opioid receptor selective, cyclic tetrapeptide dermorphin analogs: divergence from related pentapeptide enkephalin analogs. Ph.D. thesis. University of Michigan, Ann Arbor, MI.

Heyl, D. L., and H. I. Mosberg. 1992a. Modification of the nature of the Phe³ aromatic moiety in a series of delta receptor-selective dermorphin/deltorphin-related tetrapeptides: effects on opioid receptor binding. *Int. J. Pept. Protein Res.* 39:450–457.

Heyl, D. L., and H. I. Mosberg. 1992b. Substitution on the Phe³ aromatic ring in cyclic delta receptor-selective dermorphin/deltorphin tetrapeptide analogs: electronic and lipophilic requirements for receptor affinity. *J. Med. Chem.* 35:1535–1541.

Hjorth, S. A., K. Thirstrup, D. K. Grandy, and T. W. Schwartz. 1995. Analysis of selective binding epitope for the κ-opioid receptor antagonist norbinaltorphimine. *Mol. Pharmacol.* 47:1089–1094.

Ho, B. Y., A. Karschin, T. Branchek, N. Davidson, and H. A. Lester. 1992. The role of conserved aspartate and serine residues in ligand binding and function of the 5-HT₁A receptor: a site directed mutation study. *FEBS Lett.* 312:259–262.

Ho, J. 1997. Development of a model for the μ opioid receptor pharmacophore. Ph.D. thesis. University of Michigan, Ann Arbor, MI.

Housset, D., K.-S Kim,. J. Fuchs, C. Woodward, and A. Wlodawer. 1991. Crystal structure of a Y35G mutant of bovine pancreatic trypsin inhibitor. *J. Mol. Biol.* 220:757–770.

Hwa, J., R. Gaivin, J. E. Porter, and D. M. Perez. 1997. Synergism of constitutive activity in alpha-1-adrenergic receptor. *Biochemistry.* 36:633–639.

Javitch, J. A., D. Fu, J. Chen, and A. Karlin. 1995. Mapping the binding-site crevice of the dopamine D2 receptor by the substituted-cysteine accessibility method. *Neuron.* 14:825–831.

Javitch, J. A., X. Li, J. Kaback, and A. Karlin. 1994. A cysteine residue in the third membrane-spanning segment of the human D_2 dopamine receptor is exposed in the binding-site crevice. *Proc. Natl. Acad. Sci. USA.* 91:10355–10359.

Klein, C. L., R. J. Majeste, and E. D. Stevens. 1987. Experimental electron density distribution of naloxone hydrochloride dihydrate, a potent opiate antagonist. *J. Am. Chem. Soc.* 109:6675–6681.

Knapp, R. J., E. Malatynska, N. Collins, L. Fang, J. Y. Wang, V. J. Hruby, W. R. Roeske, and H. I. Yamamura. 1995. Molecular biology and pharmacology of cloned opioid receptors. *FASEB J.* 9:516–525.

Kollman, P. A. 1993. Free energy calculations: applications to chemical and biochemical phenomena. *Chem. Rev.* 93:2395–2417.

Kong, H., K. Raynor, H. Yano, J. Takeda, G. I. Bell, and T. Reisine. 1994. Agonists and antagonists bind to different domains of the cloned κ-opioid receptor. *Proc. Natl. Acad. Sci. USA.* 91:8042–8046.

Kong, H., K. Raynor, H. Yano, K. Yasuda, S. T. Moe, P. S. Portoghese, G. I. Bell, and T. Reisine. 1993. A single residue, aspartic acid 95, in the δ-opioid receptor specifies selective high affinity agonist binding. *J. Biol. Chem.* 268:23055–23058.

Lahti, R. A., M. M. Mickelson, J. M. McCall, and P. F. Von Voigtlander. 1985. [^{3}H]-U69,593, a highly selective ligand for the opioid κ-receptor. *Eur. J. Pharmacol.* 109:281–284.

Lesk, A. M., and C. Chothia. 1980. How different amino acid sequences determine similar protein structures: the structure and evolutionary dynamics of globins. *J. Mol. Biol.* 136:225–270.

Lomize, A. L., J. L. Flippen-Andersen, C. George, and H. I. Mosberg. 1994. Conformational analysis of the receptor selective, cyclic opioid peptide, Tyr-cyclo[D-Cys-Phe-D-Pen]OH (JOM-13). Comparison of x-ray crystollagraphic structures, molecular mechanics simulations, and ^{1}H NMR data. *J. Am. Chem. Soc.* 116:429–436.

Lomize, A. L., I. D. Pogozheva, and H. I. Mosberg. 1996. Development of a model for the opioid receptor pharmacophore. 3. Comparison of the cyclic tetrapeptide, Tyr-c[D-Cys-Phe-D-Phe]OH with other conformationally constrained δ-receptor selective ligands. *Biopolymers.* 38:221–234.

Lomize, A. L., I. D. Pogozheva, and H. I. Mosberg. 1998. Structural organization of G-protein-coupled receptors. *Perspect. Drug Discovery Design.* (in press).

Louie, G. V., and G. D. Brayer. 1989. A polypeptide chain-refolding event occurs in the Gly82 variant of yeast iso-1-cytochrome c. *J. Mol. Biol.* 209:313–322.

Mansour, A., F. Meng, J. H. Meador-Woodruff, L. P. Taylor, O. Civelli, and H. Akil. 1992. Site-directed mutagenesis of the human dopamine D2 receptor. *Eur. J. Pharmacol.* 227:205–214.

Mansour, A., L. P. Taylor, J. L. Fine, R. C. Thompson, M. T. Hoversten, H. I. Mosberg, S. J. Watson, and H. Akil. 1997. Key residues defining the μ opioid receptor binding pocket: a site-directed mutagenesis study. *J. Neurochem.* 68:344–353.

McDonald, I. K., and J. M. Thornton. 1994. Satisfying hydrogen bonding potential in proteins. *J. Mol. Biol.* 238:777–793.

Meng, F., M. T. Hoversten, R. C. Thompson, L. Taylor, S. J. Watson, and H. Akil. 1995. A chimeric study of the molecular basis of affinity and selectivity of the κ and the δ-opioid receptors. *J. Biol. Chem.* 270:12730–12736.

Meng, F., Y. Ueda, M. T. Hoversten, R. C. Thompson, L. Taylor, S. J. Watson, and H. Akil. 1996. Mapping the receptor domains critical for the binding selectivity of δ-opioid receptor ligands. *Eur. J. Pharmacol.* 311:285–292.

Metzger, T. G., and D. M. Ferguson. 1995. On the role of extracellular loops of opioid receptors in conferring ligand selectivity. *FEBS Lett.* 375:1–4.

Metzger, T. G., M. G. Paterline, P. S. Portoghese, and D. M. Ferguson. 1996. Application of the message-address concept to the docking of naltrexone and selective naltrexone-derived opioid antagonists into opioid receptor models. *Neurochem. Res.* 21:1287–1294.

Minami, M., T. Nakagawa, T. Seki, T. Onogi, Y. Aoki, Y. Katao, S. Katsumata, and M. Satoh. 1996. A single residue, Lys108 of the δ-opioid receptor prevents the μ-opioid selective ligand [D-Ala2,N-MePhe4,Glyol5]enkephalin from binding to the δ-opioid receptor. *Mol. Pharmacol.* 50:1413–1422.

Momany, F. A., and R. Rone. 1992. Validation of the general purpose QUANTA3.2/CHARMm force field. *J. Comput. Chem.* 13:888–900.

Mosberg, H. I., R. K. Dua, I. D. Pogozheva, and A. L. Lomize. 1996. Development of a model for the δ opioid receptor pharmacophore. 4. Residue 3 dehydrophenylalanine analogues of Tyr-*cyclo*-[D-Cys-Phe-D-Pen]OH (JOM-13) confirm required *gauche* orientation of aromatic side chain. *Biopolymers.* 39:287–296.

Mosberg, H. I., R. Hurst, V. J. Hruby, K. Gee, H. I. Yamamura, J. J. Galligan, and T. F. Burks. 1983. Bis-penicillinamine enkephalins possess highly improved specificity toward δ-opioid receptors. *Proc. Natl. Acad. Sci. USA.* 80:5871–5874.

Mosberg, H. I., A. L. Lomize, C. Wang, H. Kroona, D. L. Heyl, K. Sobczyk-Kojiro, W. Ma, C. Mousigan, and F. Porreca. 1994a. Development of a model for the δ-opioid receptor pharmacophore. 2. Conformationally restricted Tyr^1 replacements in the cyclic δ-receptor selective tetrapeptide Tyr-c[D-Cys-Phe-D-Pen]OH (JOM-13). *J. Med. Chem.* 37:4371–4383.

Mosberg, H. I., J. R. Omnaas, A. L. Lomize, D. L. Heyl, I. Nordan, C. Mousigan, P. Davis, and F. Porreca. 1994b. Development of a model for the δ-opioid receptor pharmacophore. 2. Conformationally restricted Phe^3 replacements in the cyclic δ-receptor selective tetrapeptide Tyr-c[D-Cys-Phe-D-Pen]OH (JOM-13). *J. Med. Chem.* 37:4384–4391.

Mosberg, H. I., J. R. Omnaas, C. B. Smith, and F. Medzihradsky. 1988. Cyclic disulfide- and dithioether-containing opioid tetrapeptides: development of a ligand with enhanced delta opioid receptor selectivity and potency *Life Sci.* 43:1013–1020.

Mosberg, H. I., and K. Sobczyk-Kojiro. 1991. A ^{1}H NMR study of HTyr-D-Cys-Phe-D-PenOH (JOM-13), a highly selective ligand for the delta opioid receptor. *In* Proteins. V. Renugopalakrishnan, editor. ESCOM, Leiden, the Netherlands. 105–109.

Mosberg, H. I., K. Sobczyk-Kojiro, P. Subramanian, G. M. Crippen, K. Ramalingam, and R. W. Woodard. 1990. Combined use of stereospecific deuteration, NMR, distance geometry and energy minimization for the conformational analysis of the delta opioid receptor selective peptide, [D-Pen^2,D-Pen^5]enkephalin. *J. Am. Chem. Soc* 112:822–829.

Oliveira, L., A. C. M. Paiva, and G. Vriend. 1993. A common motif in G-protein-coupled seven transmembrane helix receptors. *J. Computer-Aided Mol. Design.* 7:649–658.

Onogi, T., M. Minami, Y. Katao, T. Nakagawa, Y. Aoki, T. Toya, S. Katsumata, and M. Satoh. 1995. DAMGO, a μ-opioid receptor selective agonist, distinguishes between μ- and δ-opioid receptors around their first extracellular loops. *FEBS Lett.* 357:93–97.

Pepin, M.-C., S. Y. Yue, E. Roberts, C. Wahlestedt, and P. Walker. 1997. Novel "restoration of function" mutagenesis strategy to identify amino acids of the δ-opioid receptor involved in ligand binding. *J. Biol. Chem.* 272:9260–9267.

Pogozheva, I. D., A. L. Lomize, and H. I. Mosberg. 1997. The transmembrane 7-α-bundle of rhodopsin: distance geometry calculation with hydrogen bonding constraints. *Biophys. J.* 70:1963–1985.

Porter, J. E., J. Hwa, and D. M. Perez. 1996. Activation of the alpha-1b-adrenergic receptor is initiated by disruption of an interhelical salt bridge constraint. *J. Biol. Chem.* 45:28318–28323.

Portoghese, P. S., C.-E. Lin, F. Farour-Grant, and A. E. Takemori. 1994. Structure-activity relationship of N17′-substituted norbinaltorphimine congeners. Role of the N17′ basic group in the interaction with a putative address subsite on the κ opioid receptor. *J. Med. Chem.* 37:1495–1500.

Portoghese, P. S., A. W. Lipkowski, and A. E. Takemori. 1987. Bimorphinans as highly selective, potent kappa receptor antagonists. *J. Med. Chem.* 30:238–239.

Portoghese, P. S., M. Sultana, and A. E. Takemori. 1990. Design of peptidomimetic δ-opioid receptor antagonists using the message-address concept. *J. Med. Chem.* 33:1714–1720.

Reisine, T. 1995. Opiate receptors. *Neuropharmacology.* 34:463–472.

Richardson, J. S., and D. C. Richardson. 1989. Principles and patterns of protein conformation. *In* Prediction of Protein Structure and the Principles of Protein Conformation. G. D. Fasman, editor. Plenum Press, New York and London. 2–97.

Robinson, P. R., G. B. Cohen, E. A. Zhukovsky, and D. D. Oprian. 1992. Constitutively active mutants of rhodopsin. *Neuron.* 9:719–725.

Römer, D., H. Buscher, R. C. Hill, R. Maurer, T. J. Petcher, H. B. Welle, H. C. Bakel, A. M. Akkerman. 1980. Bremazocine: a potent, long-acting opiate kappa-agonist. *Life Sci.* 27:971–978.

Sakmar, T. P., and K. Fahmy. 1995. Properties and photoactivity of rhodopsin mutants. *Isr. J. Chem.* 35:325–337.

Savarese, T. M., and C. M. Fraser. 1992. In vitro mutagenesis and the search for structure-function relationships among G-protein-coupled receptors. *Biochem. J.* 283:1–19.

Sauer, U. H., S. Dao-pin, and B. W. Matthews. 1992. Tolerance of T4 lysozyme to proline substitutions within the long interdomain α-helix illustrates the adaptability of protein to potentially destabilizing lesions. *J. Biol. Chem.* 267:2393–2399.

Schertler, G. F. X., C. Villa, and R. Henderson. 1993. Projection structure of rhodopsin. *Nature.* 362:770–772.

Schultz, G. E. 1992. Structure-function relationships in the membrane channel porin as based on 1.8 Å resolution crystal structure. *In* Membrane Proteins: Structure, Interactions and Models. A. Pullman, J. Jortner, and B. Pullman, editors. Kluwer Academic Publishers, Dordrecht, the Netherlands. 403–412.

Sealfon, S. C., L. Chi, B. J. Ebersole, V. Rodic, D. Zhang, J. A. Ballesteros, and H. Weinstein. 1995. Related contribution of specific helix 2 and helix 7 residues to conformational activation of the serotonin 5-HT$_{2A}$ receptor. *J. Biol. Chem.* 270:16683–16688.

Shahrestanifar, M., W. W. Wang, and R. D. Howells. 1996. Studies on inhibition of μ- and δ-opioid receptor binding by dithiothreitol and *N*-ethylmaleimide. His^{223} is critical for μ-opioid binding and inactivation by *N*-ethylmaleimide. *J. Biol. Chem.* 271:5505–5512.

Sheikh, S., T. A. Zviaga, O. Lichtarge, T. P. Sakmar, and H. R. Bourne. 1996. Rhodopsin activation blocked by metal-ion-binding sites linking transmembrane helices c and F. *Nature.* 383:347–350.

Shieh, T., M. Han, T. P. Sakmar, and S. O. Smith. 1997. The steric trigger in rhodopsin activation. *J. Mol. Biol.* 269:373–384.

Sibanda, B. L., and J. M. Thornton. 1991. Conformation of β-hairpins in protein structures: classification and diversity in homologous structures. *Methods Enzymol.* 202:59–83.

Strader, C. D., M. R. Candelore, W. S. Hill, I. S. Sigal, and R. A. F. Dixon. 1989. Identification of two serine residues involved in agonist activation of the β-adrenergic receptor. *J. Biol. Chem.* 264:13572–13578.

Strader, C. D., I. S. Sigal, M. R. Candelore, E. Rands, W. S. Hill, and R. A. F. Dixon. 1988. Conserved aspartic acid residues 79 and 113 of the β-adrenergic receptor have different roles in receptor function. *J. Biol. Chem.* 263:10267–10271.

Strader, C. D., I. S. Sigal, R. B. Register, M. R. Candelore, E. Rands, and R. A. F. Dixon. 1987. Identification of residues required for ligand binding to the β-adrenergic receptor. *Proc. Natl. Acad. Sci. USA.* 84:4384–4388.

Surratt, C. K., P. S. Johnson, A. Moriwaki, B. K. Seidleck, C. J. Blaschak, J. B. Wang, and G. R. Uhl. 1994. Opiate receptor. Charged transmembrane domain amino acids are critical for agonist recognition and intrinsic activity. *J. Biol. Chem.* 269:20548–20553.

Szmuszkovicz, J., and P. F. Von Voightlander. 1982. Benzeneacetamide amines: structurally novel non-μ-opioids. *J. Med. Chem.* 25:1125–1126.

Takemori, A. E., and P. S. Portoghese. 1985. Affinity labels for opioid receptors. *Annu. Rev. Pharmacol. Toxicol.* 25:193–223.

Thirstrup, K., C. E. Elling, S. A. Hjorth, and T. W. Schwartz. 1996. Construction of a high affinity zinc switch in the κ-opioid receptor. *J. Biol. Chem.* 271:7875–7878.

Unger, V. M., P. A. Hargrave, J. M. Baldwin, and G. F. X. Schertler. 1997. Arrangement of rhodopsin transmembrane α-helices. *Nature.* 389:203–206.

Unger, V. M., and G. F. X. Schertler. 1995. Low resolution structure of bovine rhodopsin determined by electron cryo-microscopy. *Biophys. J.* 68:1776–1786.

Urbanczyk-Lipkowska, Z., and M. C. Etter. 1987. The crystal structure of a bimorphinan with highly selective kappa opioid receptor antagonist activity. *J. Mol. Struct.* 159:287–295.

Valiquette, M., H. K. Vu, S. Y. Yue, C. Wahlestedt, and P. Walker. 1996. Involvement of Trp^{284}, Val^{296}, and Val^{297} of the human δ-opioid receptor in binding of δ-selective ligands. *J. Biol. Chem.* 271:18789–18796.

Varga, E. V., X. Li, D. Stropova, T. Zalewska, R. S. Landsman, R. J. Knapp, V. J. Hruby, W. R. Roeske, and H. I. Yamamura. 1996. The third extracellular loop of the human δ-opioid receptor determines the selectivity of δ-opioid agonists. *Mol. Pharmacol.* 50:1619–1624.

Verlinde, C. L., N. M. Blaton, C. J. De Ranter, and O. M. Peeters. 1984. 5-Ethyl-2′-hydroxy-2-[(1-hydroxycyclopropyl)methyl]-9,9-dimethyl-6,7-benzomorphan hydrochloride (bremazocine). *Acta Crystallogr. C.* 40:1759–1761.

Wang, C.-D., M. A. Buck, and C. M. Fraser. 1991. Site-directed mutagenesis of α_{2A}-adrenergicreceptors: identification of amino acids involved in ligand binding and receptor activation by agonists. *Mol. Pharmacol.* 40:168–179.

Wang, C.-D., T. K. Gallaher, and J. C. Shih. 1993. Site-directed mutagenesis of the serotonin 5-hydroxytryptamine$_2$ receptor: identification of amino acid necessary for ligand binding and receptor activation. *Mol. Pharmacol.* 43:931–940.

Wang, J. B., P. S. Johnson, J. M. Wu, W. F. Wang, and G. R. Uhl. 1994. Human κ-opiate receptor second extracellular loop elevates dynorphin's affinity for human μ/κ-chimeras. *J. Biol. Chem.* 269:25966–25969.

Wang, W. W., M. Shahrestanifar, J. Jin, and R. D. Howells. 1995. Studies on the μ and δ opioid receptor selectivity utilizing chimeric and site-mutagenized receptors. *Proc. Natl. Acad. Sci. USA.* 92:12436–12440.

Watson, S., and S. Arkinstall. 1994. The G-Protein Linked Receptor Facts Book. Academic Press, San Diego. 1–294.

Wess, J., D. Gdula, and M. R. Brann. 1991. Site-directed mutagenesis of the m3 muscarinic receptor: identification of a series of threonine and tyrosine residues involved in agonist but not antagonist binding. *EMBO. J.* 10:3729–3734.

Wilkes, B., and P. Schiller. 1991. Comparative conformational analysis of [D-Pen^2,D-Pen^5]enkephalin (DPDPE): a molecular mechanics study. *J. Computer-Aided Mol. Design.* 5:293–302.

Wong, S. K.-F., C. Slaughter, A. Ruoho, and E. M. Ross. 1988. The catecholamine binding site of the β-adrenergic receptor is formed by juxtaposed membrane-spanning domains. *J. Biol. Chem.* 263:7925–7928.

Yu, H., M. Kono, T. D. McKee, and D. D. Oprian. 1995. General method for mapping tertiary contacts between amino acid residues in membrane-embedded proteins. *Biochemistry.* 34:14963–14969.

Xue, J.-C., C. Chen, J. Zhu, S. P. Kunapuli, J. K. de Riel, L. Yu, and L.-Y. Liu-Chen. 1994. Differential binding domains of peptide and non-peptide ligands in the cloned rat κ-opioid receptor. *J. Biol. Chem.* 269:30195–30199.

Xue, J.-C., C. Chen, J. Zhu, S. P. Kunapuli, J. K. de Riel, L. Yu, and L.-Y. Liu-Chen. 1995. The third extracellular loop of the μ-opioid receptor is important for agonist selectivity. *J. Biol. Chem.* 270:12977–12979.

Zaki, P. A., E. J. Bilsky, T. W. Vanderah, J. Lai, C. J. Evans, F. Porreca. 1996. Opioid receptor types and subtypes: the δ-receptor as a model. *Annu. Rev. Pharmacol. Toxicol.* 36:379–401.

Zhou, W., C. Flanagan, J. A. Ballesteros, K. Konvicka, J. S. Davidson, H. Weinstein, R. P. Millar, and S. C. Sealfon. 1994. A reciprocal mutation supports helix 2 and helix 7 proximity in the gonadotropin-releasing hormone receptor. *Mol. Pharmacol.* 45:165–170.

Zhu, J., J. Yin, P.-Y. Law, P. A. Claude, K. C. Rice, C. J. Evans, C. Chen, L. Yu, and L.-Y. Liu-Chen. 1996a. Irreversible binding of *cis*-(+)-3-methylfentanyl isothiocyanate to the δ-opioid receptor and determination of its binding domain. *J. Biol. Chem.* 271:1430–1434.

Zhu, J., J.-C. Xue, P.-Y. Law, P. A. Claude, L.-Y. Luo, J. Yin, C. Chen, and L.-Y. Liu-Chen. 1996b. The region in the μ opioid receptor conferring selectivity for sufentanil over the δ receptor is different from over the κ receptor. *FEBS Lett.* 384:198–202.

Zhukovsky, E. A., P. R. Robinson, and D. D. Oprian. 1992. Changing the location of the Schiff base counterion in rhodopsin. *Biochemistry.* 31:10400–10405.